



Robust multi-machine power system stabilizer design using bio-inspired optimization techniques and their comparison

Dhanraj Chitara^a, P.K. Singhal^a, S.L. Surana^a, Gulshan Sharma^b, R.C. Bansal^{c,d,*}

^a Department of Electrical Engineering, Swami Keshvanand Institute of Technology (SKIT), Management & Gramothan, Jaipur (Raj.), India

^b Department of Electrical Engineering Technology, University of Johannesburg, Johannesburg, 2006, South Africa

^c Department of Electrical Engineering, University of Sharjah, Sharjah, United Arab Emirates

^d Department of Electric, Electronic and Computer Engineering, University of Pretoria, Pretoria, South Africa

ARTICLE INFO

Keywords:

Low-frequency Oscillations
Power System Stabilizer
Grey Wolf Optimization
Sooty-Tern Optimization

ABSTRACT

This paper reports a comparative study among four bio-inspired meta-heuristic techniques i.e. Sooty-Tern Optimization (STO), Grey Wolf Optimization (GWO), Genetic Algorithm (GA), and Particle Swarm Optimization (PSO) to tune the robust Power System Stabilizer (PSS) parameters of the multi-machine power system. These approaches are successfully tested on two bench-mark systems: sixteen-machine, sixty-eight-bus New England Extended Power Grid (NEEPG) and three-machine, nine-bus Western System Coordinating Council (WSCC). The efficacy of planned PSS via STO and GWO is validated by extensive non-linear simulations, eigenvalue analysis, and performance indices for numerous operating conditions under decisive perturbations, and outcomes are matched with those of GA and PSO techniques. In addition, the robustness is also tested for these algorithms. The results indicate that the PSS design using STO and GWO improves the small-signal stability and damping performance for mitigating inter-area and local area modes of low-frequency oscillations compared to GA and PSO.

1. Introduction

In the recent past, the Small-Signal Stability (SSS) of Multi-Machine Power Systems (MMPS) has become a bigger challenge for engineers. The SSS concerns low-frequency electromechanical oscillations that arise due to unbalance between mechanical and electrical torques at synchronous generators after small perturbations [1]. These disturbances cause system separation, endangering system security, and power transfer capability, creates stress on the mechanical shaft, and decrease the overall operating efficiency of the power system if tolerable damping is not introduced. As per the literature, these oscillations in MMPS are inter-area and local areas [1,2]. To boost the damping performance and SSS, Power System Stabilizers (PSSs) are adopted to damp such oscillations via excitation control of synchronous generator [3]. However, in [3], it is mentioned that the proper tuning of PSS parameters plays a vital role in performance during the system perturbation. Literature reveals that the Conventional PSSs (CPSS) have been employed as effective damping controllers in power systems due to their simplicity and satisfactory performance [2,3]. The CPSS designs are

based on the linearized theory of control system that helps to mitigate the low-frequency oscillations efficiently only for a specific operating point. The CPSS designs are unsuccessful for a variation in the extensive range of operating settings of non-linear power systems. Although, classical control techniques like root-locus [4], frequency response [5], digital control [6], pole-placement [7], non-linear & adaptive control methods [8,9], etc. perform satisfactorily but are not appropriate for non-convex and non-differentiable problem functions.

With the development of the power system, complication in the systems has increased enormously. As a result of this analysis of power systems by conventional methods has become very complicated, difficult, and time-consuming. Now, Artificial Intelligence (AI) based methods like fuzzy logic, artificial neural network, and combined neuro-fuzzy [10–12] have emerged as active tools to resolve the issue of low-frequency oscillation. The advantages of AI methods are fast processing speed, more robustness, fault-tolerant capability, and can handle conditions of incomplete information about data and corrupt data. In the literature, it is seen that the optimization methods are categorized into two major groups namely, mathematics-based classical techniques and

* Corresponding author at: Department of Electrical Engineering, University of Sharjah, Sharjah, United Arab Emirates.

E-mail addresses: dhanraj.chitara@skit.ac.in (D. Chitara), prateek.singhal@skit.ac.in (P.K. Singhal), sls@skit.ac.in (S.L. Surana), gulshans@uj.ac.za (G. Sharma), rcbansal@ieee.org (R.C. Bansal).

<https://doi.org/10.1016/j.ijepes.2023.109615>

Received 23 June 2023; Received in revised form 2 October 2023; Accepted 23 October 2023

Available online 16 November 2023

0142-0615/© 2023 Published by Elsevier Ltd. This is an open access article under the CC BY-NC-ND license (<http://creativecommons.org/licenses/by-nc-nd/4.0/>).

Table 1

Performance of optimization techniques in PSS design.

Year	Optimization Technique	Problem Solutions
1996	Genetic Algorithm (GA) [13]	PSS designed for Single Machine Infinite Bus (SMIB) system for some operating cases
1999	Tabu Search (TS) Algorithm [14]	PSS designed for specific operating cases of SMIB system and MMPS using minimization of eigenvalue based single objective function.
2000	Simulated Annealing (SA) Algorithm [15]	PSS designed for specific operating cases of MMPS using minimization of eigenvalue based single objective function.
2002	Particle Swarm Optimization (PSO) Algorithm [16]	PSS designed for specific operating cases of MMPS using minimization of eigenvalue based multi-objective function.
2002	Evolutionary Programming Algorithm [17]	PSS designed for specific operating cases of MMPS using minimization of squared eigenvalue based single-objective function.
2007	Bacteria Forging Algorithm (BFA) [18]	PSS designed for specific operating cases of MMPS using minimization of squared eigenvalue based single and multi-objective functions.
2010	Chaotic Algorithm (CA) [19]	PSS designed for specific operating cases of MMPS using minimization of squared eigenvalue based multi-objective function.
2012	Ant Colony Algorithm [20]	PSS designed for specific operating cases of MMPS using minimization of squared eigenvalue based multi-objective function and results compared with GA, PSO and CA.
2013	Cultural Algorithm [21]	PSS designed for specific operating cases of MMPS using minimization of squared eigenvalue based multi-objective function and results compared with GA.
2014	Bat Algorithm (BA) [22]	PSS designed for specific operating cases of MMPS using minimization of squared eigenvalue based multi-objective function and results compared with GA and CPSS.
2015	Orthogonal Learning Artificial Bee Colony (ABC) Algorithm [23]	PSS designed for specific operating cases of SMIB system using minimization of speed deviation based objective function and results compared with ABC and CPSS.
2016	Chaotic Teaching Learning Algorithm (TLA) [24]	PSS designed for specific operating cases of MMPS using minimization of speed deviation based objective function and results compared with GA and TLA.
2016	Cuckoo Search Algorithm [25]	PSS designed for specific operating cases of MMPS using minimization of squared eigenvalue based multi-objective function and results compared with GA and CPSS.
2017	Back Tracking Search Algorithm [26]	PSS designed for specific operating cases of MMPS using minimization of squared eigenvalue based multi-objective function and results compared with PSO and BFA.
2018	Salap Swarm Algorithm (SSA) [27]	PSS designed for specific operating cases of MMPS using minimization of squared eigenvalue based multi-objective function and results compared with TS.
2018	Ant Lion Algorithm [28]	PSS designed for specific operating cases of MMPS using minimization of speed deviation based objective function and results compared with PSO and SSA.
2019	Hyper-Spherical Search Algorithm [29]	PSS designed for specific operating cases of MMPS using minimization

Table 1 (continued)

Year	Optimization Technique	Problem Solutions
		of speed deviation based objective function and results compared with GA and CPSS.
2020	Slime Mould Algorithm [30]	PSS designed for specific operating cases of SMIB system using minimization of squared eigenvalue based multi-objective function and results compared with GA.
2021	Henry Gas Solubility Algorithm [31]	PSS designed for specific operating cases of SMIB system using minimization of speed deviation based objective function and results compared with Atomic Search Optimization (ASO).
2021	Harris Hawk Optimization Algorithm [32]	PSS designed for specific operating cases of MMPS using maximization of damping ratio based objective function and results compared with differential evolution.
2022	Reptile Search Algorithm (RSA) [33]	PSS designed for specific operating cases of SMIB system and MMPS using minimization of speed deviation based objective function and results compared with GA and BA.
2022	Improved Atomic Search Optimization (IASO) Algorithm [34]	PSS designed for specific operating cases of SMIB system using minimization of speed deviation based objective function and results compared with GA, PSO, SA and ASO.
2022	Hybrid Water Cycle Moth-Flame Optimization Algorithm [35]	PSS designed for specific operating cases of SMIB system using minimization of speed deviation based objective function and results compared with water cycle algorithm, moth-flame optimization and artificial ecosystem optimization.
2022	Rat Swarm Optimization Algorithm [36]	PSS designed for specific operating cases of MMPS using minimization of squared eigenvalue based multi-objective function and results compared with CPSS.
2022	Revamped Sine Cosine Algorithm [37]	PSS and POD designed for specific operating cases of MMPS with DF IG using minimization of squared eigenvalue based multi-objective function and results compared with whale optimization algorithm.
2023	Weighted Mean of Vectors Algorithm [38]	PSS designed for specific operating cases of SMIB system using minimization of speed deviation based objective function and results compared with grey wolf optimization, BA, RSA and IASO.
2023	Mayfly Algorithm [39]	PSS designed for specific operating cases of MMPS using maximization of damping ratio based objective function and results compared with firefly algorithm and PSO.
2023	Hybrid Gorilla Troops Optimization (GTO) and Gradient-Based Optimization (GBO) Algorithm [40]	PSS designed for specific operating cases of MMPS using maximization of damping ratio based objective function and results compared with AEO, GTO and GBO.

meta-heuristic techniques. Performance of optimization techniques employed in literature for PSS designing are depicted in Table 1.

However, the meta-heuristic techniques suffer from the issue of high run time, and slow convergence depending on the system size under study, but these are off-line techniques and free from mathematical modelling. The main advantage of meta-heuristic techniques is that they are based on evolutionary schemes and information exchange between

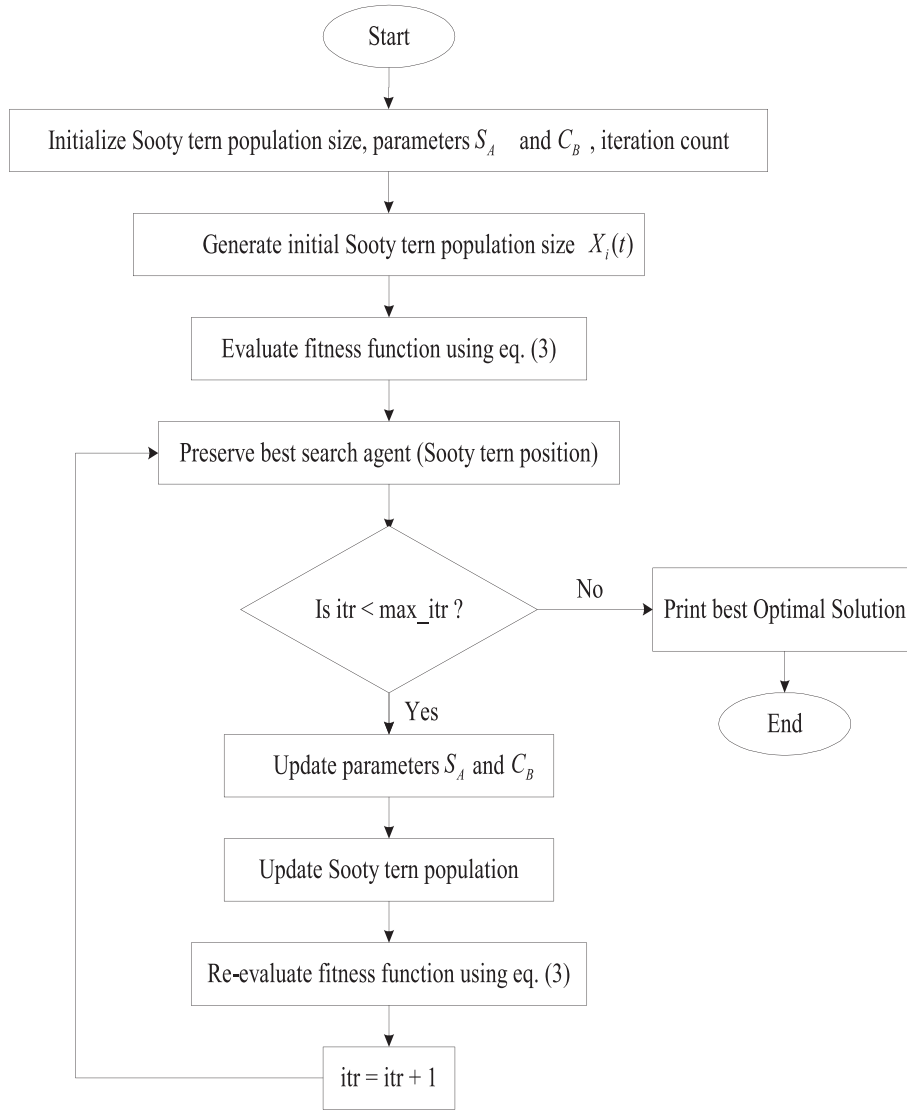


Fig. 1. Flow Chart of STO.

individuals.

In this paper, four bio-inspired optimization techniques: Sooty-Tern Optimization (STO) [41], GWO [42], GA [43], and PSO [44] techniques have been explored for designing the PSS of MMPS. The tuning procedure is modeled as a multi-objective based on eigenvalue modes optimization problem for relocating the unstable right-half of s-plane eigenvalues to a definite stable D-shape sector in the left-half of the s-plane. To depict the performance of the designed PSS, these algorithms are successfully tested on two benchmark test systems: sixteen-machine, sixty-eight-bus New England Extended Power Grid (NEEPG) and three-machine, nine-bus Western System Coordinating Council (WSCC) for various operating cases under decisive perturbations. The effectiveness of tuned PSS is checked by non-linear simulations, performance indices: Integral of Absolute Error (IAE) & Integral of Time-Absolute Error (ITAE), and eigenvalue analysis using the Power System Analysis Toolbox (PSAT) [45] and matched with each other. The results depict the hat designed STO-stabilizer guarantees to produce robust damping performance for an extensive variety of operating settings as well as hidden operating cases also under critical disturbance as compared to GA-stabilizer, PSO-stabilizer and GWO-stabilizer. The key feature of this paper is that the designed parameters of PSS using all algorithms for selected operating cases show the robustness performance by testing them under critical disturbance for other severe operating cases also.

2. Formulation of problem

2.1. Model of power system

In this work, every generator is modelled as a two-axis, fourth-order model. For all selected operating settings, the power system can be modelled as a set of non-linear differential equations given by

$$\dot{X} = f(X, U) \quad (1)$$

where state vector $X = [\delta, w, E'_q, E_{fd}]^T$ is a set of variables: rotor angle δ , rotor speed w , internal voltage E'_q and the field voltage E_{fd} respectively and input variables vector U . Moreover, the system is assumed to be a linearized incremental model around a particular operating point which is commonly utilized for designing of PSS [17–22].

2.2. Modelling of PSS

The elementary task of PSS is to utilize an auxiliary stabilizing signal that helps in providing damping for generator rotor oscillations by regulating its field excitation. To offer sufficient damping, PSS produces a constituent of electrical torque in phase with rotor speed deviations [17–40]. The basic transfer function of PSS includes (i) damping

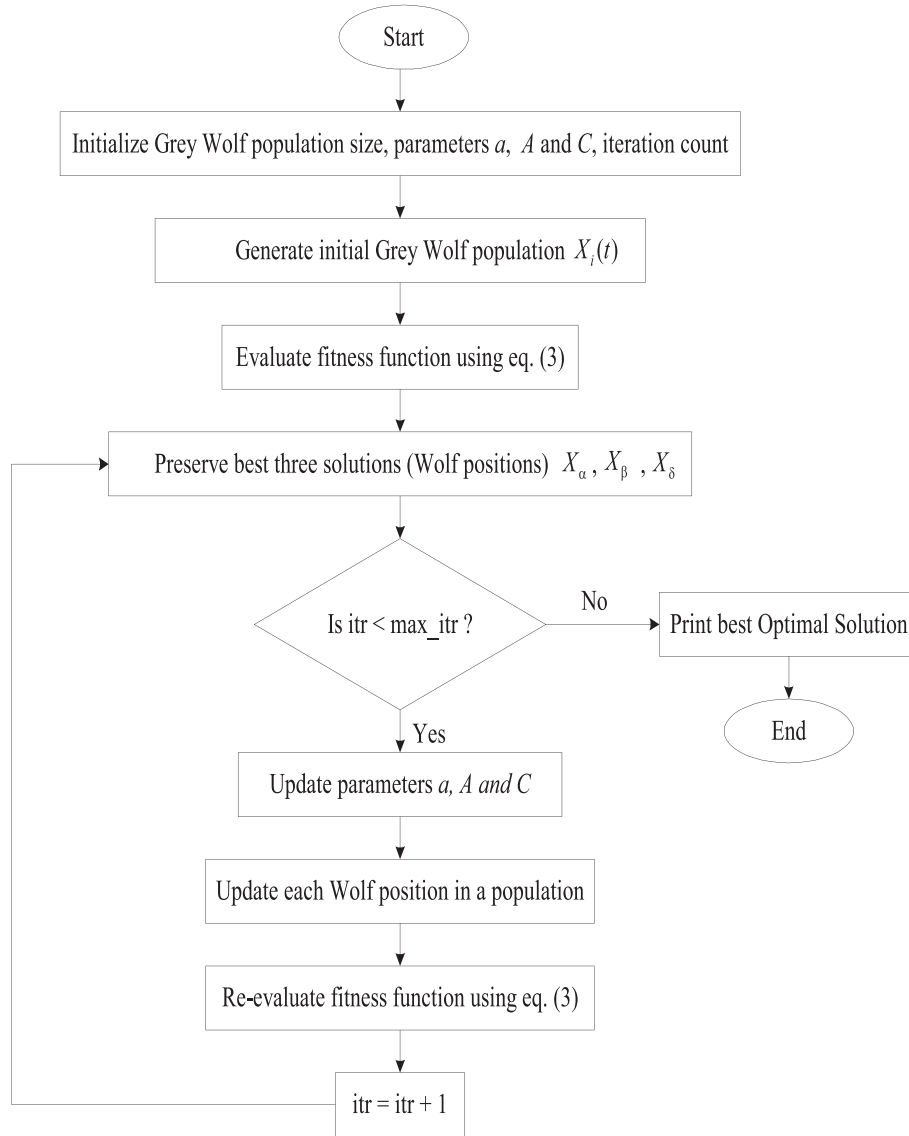


Fig. 2. Flow Chart of GWO.

Table 2
Three Generator and Load Operating Cases of WSCC Power System [25].

Operating Cases		Generator			Load			
		G_1	G_2	G_3	A	B	C	Load at G_1
Normal Loading	P	0.71	1.63	0.06	1.25	0.90	1.00	1.00
	Q	0.62	0.85	-0.10	0.50	0.30	0.35	0.35
Light Loading	P	0.96	1.00	0.45	0.70	0.50	0.60	0.60
	Q	0.22	-0.19	-0.26	0.35	0.30	0.20	0.20
Heavy Loading	P	3.57	2.20	0.71	2.00	1.80	1.60	1.60
	Q	1.81	1.35	0.43	0.90	0.60	0.65	0.65

Table 3
Six Operating Conditions of NEEPG [49].

Cases	Operating Conditions
Case-1	Nominal generation and load
Case-2	Transmission line 1–2 out of service
Case-3	Transmission line 1–27 out of service
Case-4	Transmission line 8–9 out of service
Case-5	Enhance 20 % load at bus-17
Case-6	Transmission line 46–49 out of service with load enhanced by 25 % at bus-20, 21 and generation raised by 20 % at G_9

controller gain (ii) washout time constant (iii) two stages lag-lead compensator. The standard transfer function of PSS is specified as:

$$\Delta U_i = K_i \left[\frac{sT_w}{1+sT_w} \right] \left[\frac{(1+sT_{1i})(1+sT_{3i})}{(1+sT_{2i})(1+sT_{4i})} \right] \Delta w_i \quad (2)$$

The phase lead block provide necessary phase lag compensation

between excitation input and electrical torque output for a wide range of inter-area and local area modes of oscillations. The main design problem of PSS involves the proper selection of dynamic gain K_i and time coefficients T_w , T_{1i} , T_{2i} , T_{3i} , and T_{4i} for i th machine. For the sake of simplicity, the numerical values of T_w , T_{2i} , and T_{4i} are preferred as fixed constant value while other parameters K_i and T_{1i} and T_{3i} values are to be

Table 4

Eigenvalues Analysis without PSS for Three Loading Cases of WSCC System.

Cases	Eigenvalues	Damping Ratio (%)	Frequency (p. u.)	Participation Factor	Participation Modes
Normal Loading	$-0.110 \pm j 8.588$	12.0	1.366	0.290	w_2, δ_2
	$-0.653 \pm j 13.023$	5.02	2.072	0.374	w_3, δ_3
Light Loading	$-0.637 \pm j 8.515$	7.40	1.355	0.278	w_2, δ_2
	$-1.274 \pm j 12.752$	9.90	2.029	0.355	w_3, δ_3
Heavy Loading	$0.158 \pm j 8.372$	- 1.80	1.332	0.288	w_2, δ_2
	$-0.308 \pm j 12.896$	2.40	2.052	0.384	w_3, δ_3

Table 5

Eigenvalues Analysis without PSS for Six Operating Cases of NEEPG System.

Cases	Eigenvalues & Percentage Damping Ratio	Frequency (p. u.)	Participation Factor	Participation Modes
Case-1	$0.388 \pm j 6.439, -6.02 \%$	1.024	0.350	w_9, δ_9
	$0.030 \pm j 6.662, -0.45 \%$	1.060	0.189	w_2, δ_2
	$0.009 \pm j 11.306, -0.085 \%$	1.799	0.440	w_{11}, δ_{11}
Case-2	$0.358 \pm j 6.411, -5.58 \%$	1.020	0.325	w_9, δ_9
	$0.032 \pm j 6.658, -0.48 \%$	1.059	0.195	w_2, δ_2
	$0.023 \pm j 11.248, -0.20 \%$	1.790	0.442	w_{11}, δ_{11}
Case-3	$0.382 \pm j 6.428, -5.94 \%$	1.023	0.348	w_9, δ_9
	$0.030 \pm j 6.661, -0.45 \%$	1.060	0.195	w_2, δ_2
	$0.012 \pm j 11.306, -0.11 \%$	1.799	0.440	w_{11}, δ_{11}
Case-4	$0.410 \pm j 6.400, -6.39 \%$	1.018	0.363	w_9, δ_9
	$0.016 \pm j 6.450, -0.26 \%$	1.026	0.192	w_2, δ_2
	$0.017 \pm j 11.285, -0.15 \%$	1.796	0.439	w_{11}, δ_{11}
Case-5	$0.387 \pm j 6.437, -6.00 \%$	1.024	0.350	w_9, δ_9
	$0.031 \pm j 6.663, -0.47 \%$	1.060	0.196	w_2, δ_2
	$0.014 \pm j 11.315, -0.12 \%$	1.800	0.441	w_{11}, δ_{11}
Case-6	$0.585 \pm j 6.312, -9.23 \%$	1.004	0.342	w_9, δ_9
	$0.017 \pm j 6.666, -0.26 \%$	1.061	0.192	w_2, δ_2
	$0.010 \pm j 11.284, -0.08 \%$	1.795	0.437	w_{11}, δ_{11}

evaluated [17–40].

2.3. Optimization problem

For simultaneous regulation of both damping ratio and real-part of eigenvalues, the tuned parameters of PSS may be planned to minimize the following multi-objective function in such a way that the eigenvalues of MMPS with planned PSS are significantly relocated in a D-shape sector of the stable zone in the s -plane [17–22,25–27,30,36,37].

$$J = \sum_{j=1}^{np} \sum_{\sigma_{ij} \geq \sigma_0} (\sigma_0 - \sigma_{ij})^2 + \sum_{j=1}^{np} \sum_{\xi_{ij} \leq \xi_0} (\xi_0 - \xi_{ij})^2 \quad (3)$$

where np , ξ_0 , σ_0 , ξ_{ij} and σ_{ij} are the number of operating cases to be selected, chosen damping ratio, chosen damping factor, the damping ratio and the real-part of the i th eigenvalue mode of the j th operating case respectively.

Minimize J subject to:

$$K_i^{\min} \leq K_i \leq K_i^{\max} \quad (4)$$

$$T_{li}^{\min} \leq T_{li} \leq T_{li}^{\max} \quad (5)$$

$$T_{3i}^{\min} \leq T_{3i} \leq T_{3i}^{\max} \quad (6)$$

where T_{ji}^{\max} and T_{ji}^{\min} the upper and lower bounds of time-coefficients of PSS design, K_i^{\max} and K_i^{\min} are upper and lower bounds of PSS design gain.

3. Meta-heuristic optimization techniques

3.1. Sooty-term optimization algorithm

Sooty terns named as onychoprion fucatus are the sea birds which are found on banks of the oceans proposed by Gaurav Dhiman et al [41]. These sooty terns are found in broad range and groups, with various sizes and mass. These terns are omnivores which eat fish, spiders, earthworms, reptiles, amphibians and likewise little insects of ocean. Sooty tern is a very shrewd bird that lures earthworms which are deep beneath the soil by making a rain-like noise with the feet and use bread crumbs to lure fish around. Mostly these birds spend their lives in the groups. Knowledge is shared by ranging and assaulting the prey. The most important thing of sooty terns is to migrate and assaulting actions. Immigration is known as seasonal shifting of sooty terns from one location to another for exploring the wealthiest and most plentiful areas of resources which will supply enough food and power [41]. Hunting process of sooty bird can be understood as follows:

1. Sooty terns fly in a flock throughout immigration. The primary location of sooty terns goes varying to discourage collision in between them.
2. Sooty terns fly as a team towards the best sooty terns direction, so that the sooty tern having lowest fitness level can also travel to the best solution.
3. Remaining sooty terns will change their places according to the fittest one.

The execution of the STO algorithm for tuning the PSS parameters are described as shown in Fig. 1 through the flow chart representation:

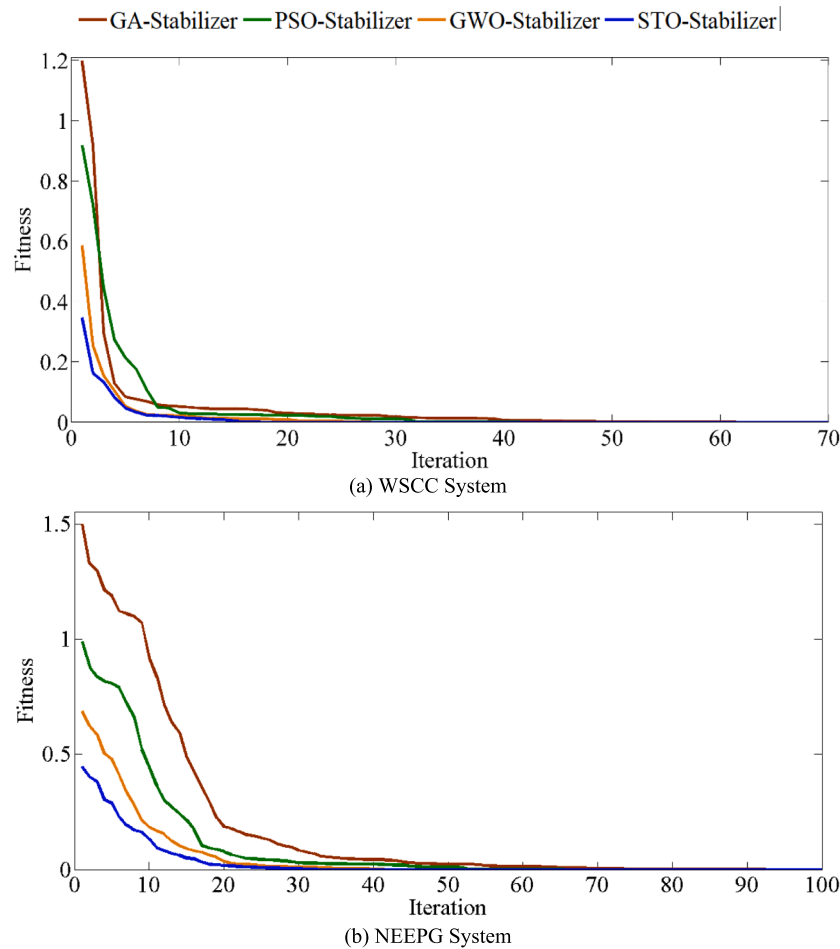


Fig. 3. Convergence Characteristics of various optimization techniques for (a) WSCC System (b) NEEPG System.

Table 6

Statistical Results of GA, PSO, GWO and STO Algorithm for WSCC and NEEPG System.

		Desired Solution Iteration	Convergence Time (sec)	Best Fitness	Average Fitness
For WSCC System	GA	62	629	0	0
	PSO	42	458	0	0
	GWO	28	321	0	0
	STO	18	258	0	0
For NEEPG System	GA	93	2758	0	0
	PSO	65	2146	0	0
	GWO	42	1863	0	0
	STO	32	1582	0	0

Table 7

Optimized Parameters of GA-stabilizer, PSO-stabilizer, GWO-stabilizer and STO-stabilizer for WSCC system.

	Generators	GA-stabilizer [47]	PSO-stabilizer [47]	GWO-stabilizer [47]	STO-stabilizer
K	G_2	1.000	1.000	5.372	3.370
	G_3	1.000	1.000	1.000	1.000
T_1	G_2	0.464	1.000	0.355	0.212
	G_3	0.610	0.400	0.155	0.180
T_3	G_2	0.060	0.156	1.000	0.060
	G_3	0.679	0.06	0.060	0.102

3.2. Grey Wolf Optimization algorithm

The Grey Wolf Optimization (GWO) technique was created by usual behavior of wolf pack and developed by Mirjalili et al [42]. Grey wolf is the apex predator in food chain and devote life in the groups. They have preserved a harsh community behavior and work in a group. They are characterized into four brands as: Alpha, Beta, Delta, and Omega based on their role played in hunting. The three main stages of hunting are look for prey, surrounding prey and aggressive prey [42]. The key merits of GWO are that it has very less parameters to be tuned and also do not require any derivative information during initialization. The execution of the GWO algorithm for tuning the PSS parameters are described as

shown in Fig. 2 through the flow chart representation:

4. Design and simulation results of PSS

4.1. Three-machine, nine-bus WSCC power system

The layout of a well-known 3-machine, 9-bus WSCC system and its data are specified in [46]. All three generators of WSCC power system are modelled as: fourth order with static exciter and constant impedance loads. Table 2 shows three different operating cases for which the study is carried out [25].

Table 8

Optimized Parameters of GA-stabilizer, PSO-stabilizer, GWO-stabilizer, and STO-stabilizer for NEEPG System.

	With GA-stabilizer			With PSO-stabilizer			With GWO-stabilizer			With STO-stabilizer		
	K_I	T_I	T_3	K_I	K_I	K_I	K_I	T_I	T_3	K_I	T_I	T_3
G_1	76.425	0.162	0.888	31.388	0.785	0.501	76.499	0.105	0.906	68.815	0.254	1.000
G_2	26.315	0.551	0.510	59.808	0.100	0.345	42.591	0.261	0.563	40.920	0.092	0.352
G_3	47.143	0.323	0.572	30.629	0.763	0.010	22.364	0.863	0.642	37.496	0.209	0.076
G_4	17.558	0.994	0.509	23.942	0.100	0.100	27.451	0.511	0.267	18.839	0.235	0.072
G_5	59.035	0.281	0.329	63.755	0.100	0.281	23.563	0.653	0.823	8.043	0.201	0.699
G_7	10.756	0.814	0.677	13.813	0.913	0.693	100.00	0.229	0.435	96.216	0.085	0.306
G_8	52.683	0.431	0.109	44.771	0.772	0.163	18.225	0.418	0.767	15.662	1.000	0.301
G_9	26.648	0.520	0.489	44.431	0.709	0.329	50.159	0.430	0.213	19.437	0.684	0.219
G_{10}	75.727	0.549	0.245	29.253	0.826	0.813	8.279	0.242	1.000	60.817	0.150	0.855
G_{11}	15.281	0.310	0.249	12.186	0.564	0.615	35.328	0.162	0.124	7.897	0.064	1.000
G_{12}	4.496	0.766	0.687	88.476	0.100	0.594	67.328	0.071	0.382	8.664	0.632	0.158
G_{13}	37.969	0.512	0.235	52.810	0.100	0.325	23.146	0.116	0.502	42.864	0.3847	0.305
G_{15}	38.367	0.388	0.263	13.955	0.766	0.297	31.542	0.580	0.152	100.000	0.397	0.266
G_{16}	42.826	0.478	0.878	26.569	0.100	0.100	74.559	0.329	0.269	60.784	1.000	0.373

Table 9

Eigenvalues Analysis with Designed GA-stabilizer, PSO-stabilizer, GWO-stabilizer, STO-stabilizer for Three Loading Cases of WSCC System.

	Normal loading	Light Loading	Heavy Loading
With GA-stabilizer [47,28]	$-1.778 \pm j 8.323$, 20.9 % $-1.887 \pm j 7.160$, 25.4 %	$-1.659 \pm j 7.724$, 21.0 % $-2.811 \pm j 7.480$, 35.1 %	$-0.961 \pm j 7.148$, 13.3 % $-1.930 \pm j 8.508$, 22.1 %
With PSO-stabilizer [47,28]	$-1.212 \pm j 7.549$, 15.8 % $-2.007 \pm j$ 14.393, 13.8 %	$-1.614 \pm j 7.563$, 20.8 % $-2.669 \pm j$ 14.041, 35.1 %	$-0.768 \pm j 7.381$, 10.3 % $-1.570 \pm j$ 14.157, 11.0 %
With GWO-stabilizer [47]	$-2.008 \pm j 7.363$, 26.3 % $-2.619 \pm j$ 17.189, 15.0 %	$-2.235 \pm j 7.598$, 28.2 % $-3.351 \pm j$ 17.010, 19.3 %	$-1.561 \pm j 7.244$, 21.0 % $-1.944 \pm j$ 17.526, 11.0 %
With STO-stabilizer	$-1.945 \pm j$ 12.189, 15.7 % $-2.135 \pm j$ 17.161, 12.3 %	$-2.719 \pm j$ 11.675, 22.6 % $-2.658 \pm j$ 16.729, 15.6 %	$-2.284 \pm j$ 17.348, 13.0 % $-1.518 \pm j$ 12.520, 12.0 %

4.2. New England Extended power Grid (NEEPG) system comprising of 16-Machine, 68-Bus

Layout of standard sixteen-machine, sixty-eight-bus New England Extended Power Grid (NEEPG) and its data are given in [48], [49]. Table 3 presents six different operating cases including under brutal and decisive line outage condition for which the study is carried out [24].

4.3. Eigenvalue analysis without PSS

The participation factor [50] can be used to identify the various modes of oscillations and their detail data for unstable and/or marginally stable modes of three loading cases of WSCC system and six operating cases of NEEPG system are depicted in Tables 4 and 5 respectively.

On analysing Table 4, it is observed that WSCC system is characterized by two local-area modes and is unstable due to large value of negative percentage damping ratio under heavy loading case as compared to other operating cases. Thus, according to high participation factor [50] of two-generators G_2 , G_3 , they were equipped with PSS for inserting damping to local area modes.

On analysing Table 5, it is observed that NEEPG system has three inter-area modes, eleven local-area modes and is unstable due to three-pairs of eigenvalues modes with negative damping for the chosen six-operating cases. Moreover, the operating Case-6 is extremely unstable

Table 10

Eigenvalues Analysis with GA-stabilizer, PSO-stabilizer, GWO-stabilizer, and STO-stabilizer, for six-operating cases of NEEPG System.

Cases	With GA-stabilizer	With PSO-stabilizer	With GWO-stabilizer	With STO-stabilizer
Case-1	$-0.940 \pm j$ 7.086, 3.1 % $-0.744 \pm j$ 3.996, 18.3 % $-0.601 \pm j$ 2.214, 26.2 %	$-1.109 \pm j$ 10.400, 10.6 % $-1.059 \pm j$ 6.923, 15.1 % $-0.641 \pm j$ 2.628, 23.6 %	$-0.894 \pm j$ 7.047, 12.5 % $-1.772 \pm j$ 12.969, 13.5 % $-0.827 \pm j$ 3.998, 20.2 %	$-0.586 \pm j$ 3.670, 15.7 % $-1.824 \pm j$ 11.300, 15.9 % $-2.073 \pm j$ 10.421, 19.5 %
Case-2	$-0.969 \pm j$ 7.081, 13.5 % $-0.750 \pm j$ 3.996, 18.4 % $-0.655 \pm j$ 2.214, 28.3 %	$-1.127 \pm j$ 10.395, 10.7 % $-1.106 \pm j$ 6.927, 15.7 % $-0.673 \pm j$ 2.595, 25.1 %	$-0.920 \pm j$ 7.039, 12.9 % $-0.830 \pm j$ 3.980, 20.4 % $-0.694 \pm j$ 2.112, 31.2 %	$-0.589 \pm j$ 3.669, 15.91 % $-1.837 \pm j$ 11.290, 16.0 % $-1.248 \pm j$ 7.014, 17.5 %
Case-3	$-0.946 \pm j$ 7.081, 13.2 % $-0.746 \pm j$ 3.992, 18.3 % $-0.645 \pm j$ 2.218, 27.9 %	$-1.113 \pm j$ 10.393, 10.6 % $-1.069 \pm j$ 6.915, 15.2 % $-0.640 \pm j$ 2.624, 23.7 %	$-0.899 \pm j$ 7.040, 12.6 % $-1.759 \pm j$ 13.055, 13.3 % $-0.825 \pm j$ 3.986, 20.2 %	$-0.585 \pm j$ 3.668, 15.7 % $-1.828 \pm j$ 11.295, 15.9 % $-1.224 \pm j$ 6.987, 17.2 %
Case-4	$-0.959 \pm j$ 7.089, 13.4 % $-0.746 \pm j$ 3.994, 18.3 % $-0.652 \pm j$ 2.225, 28.1 %	$-1.124 \pm j$ 10.407, 10.7 % $-1.103 \pm j$ 6.948, 15.6 % $-0.679 \pm j$ 2.595, 25.3 %	$-0.913 \pm j$ 7.048, 12.8 % $-1.765 \pm j$ 13.085, 13.3 % $-0.824 \pm j$ 3.989, 20.2 %	$-0.585 \pm j$ 3.672, 15.7 % $-1.809 \pm j$ 11.282, 15.8 % $-1.261 \pm j$ 7.070, 17.5 %
Case-5	$-0.941 \pm j$ 7.086, 13.1 % $-0.744 \pm j$ 3.997, 18.3 % $-0.601 \pm j$ 2.215, 26.2 %	$-1.110 \pm j$ 10.398, 10.6 % $-1.060 \pm j$ 6.923, 15.1 % $-0.640 \pm j$ 2.629, 23.6 %	$-0.895 \pm j$ 7.047, 12.6 % $-1.760 \pm j$ 13.064, 13.3 % $-0.827 \pm j$ 3.999, 20.2 %	$-0.586 \pm j$ 3.671, 15.7 % $-1.825 \pm j$ 11.298, 15.9 % $-1.213 \pm j$ 6.989, 17.1 %
Case-6	$-0.939 \pm j$ 7.105, 13.1 % $-0.761 \pm j$ 3.953, 18.9 % $-0.623 \pm j$ 2.186, 27.4 %	$-1.111 \pm j$ 10.483, 10.5 % $-1.047 \pm j$ 6.959, 14.8 % $-0.639 \pm j$ 2.635, 23.5 %	$-0.893 \pm j$ 7.068, 12.5 % $-1.768 \pm j$ 13.042, 13.4 % $-0.847 \pm j$ 3.948, 20.9 %	$-0.594 \pm j$ 3.608, 16.2 % $-1.776 \pm j$ 11.359, 15.4 % $-1.179 \pm j$ 7.000, 16.6 %

owing to large value of negative percentage damping ratio in comparison to other operating cases. Thus, according to high participation factor [50], fourteen-generators except G_6 and G_{14} were equipped with PSS to insert damping for both inter and local area modes.

• No-Stabilizer * GA-Stabilizer x PSO-Stabilizer + GWO-Stabilizer o STO-Stabilizer

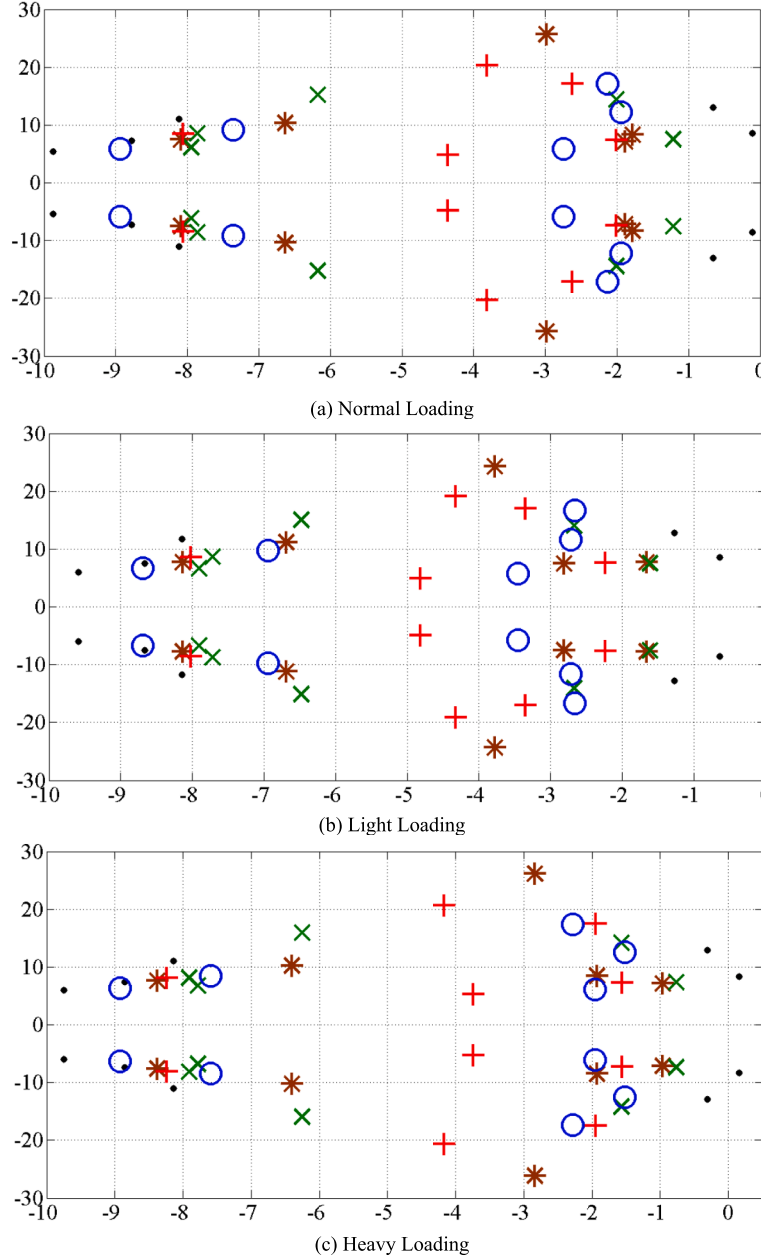


Fig. 4. Eigenvalue Map analysis with No-PSS and Designed PSS for three loading cases of WSCC System.

4.4. Eigenvalue analysis with designed PSS

To stabilize the systems, six-PSS parameters of WSCC system and forty-two parameters of NEEPG system are designed considering by minimization of objective function J depicted in equation (3) using GA, PSO, GWO and STO techniques. For both case studies, real-part of eigenvalues σ_0 is set as -0.5 and damping ratio ξ_0 is set as 10% . The target value of $J = 0$ causes the system either unstable or marginally stable. Eigenvalue modes of the system are relocated to a desired D-shape stable sector in left-half of s -plane to assure the system stability. Hence, for optimizing six-PSS parameters of WSCC system and forty-two parameters of NEEPG system, the gain K_i of PSS is varied from 1 to 100 and, the lower and upper bounds of T_{1i} and T_{3i} are set at 0.01 and 1.0 respectively [25]. To reduce the computation burden, the washout time constants T_w , T_2 and T_4 are kept constant at 5 sec, 0.05 sec and 0.05 sec respectively. The control parameters of GA, PSO, GWO and STO algorithm are

depicted in the Appendix. Typical convergence of GA-stabilizer, PSO-stabilizer, GWO-stabilizer and STO-stabilizer for WSCC system and NEEPG system are illustrated in Fig. 3 (a) and (b) respectively.

Fig. 3 shows that all algorithms are capable to discover the desired solution for which fitness function J is zero. The figure shows that the STO algorithm discover the best solution at a faster rate compared with that for GWO, PSO, and GA for WSCC system and NEEPG system. The statistical results of GA, PSO, GWO and STO Algorithm for WSCC and NEEPG System are depicted in Table 6.

The final optimized 6-parameters of WSCC and 42 parameters of NEEPG systems using GA-stabilizer, PSO-stabilizer, GWO-stabilizer, and STO-stabilizer are listed in Tables 7 and 8 respectively. The assessment of eigenvalues and percentage damping ratio with planned GA-stabilizer, PSO-stabilizer, GWO-stabilizer and STO-stabilizer for three-operating cases of WSCC system and six-operating cases of NEEPG system are listed in Tables 9 and 10 respectively. Eigenvalue map analysis

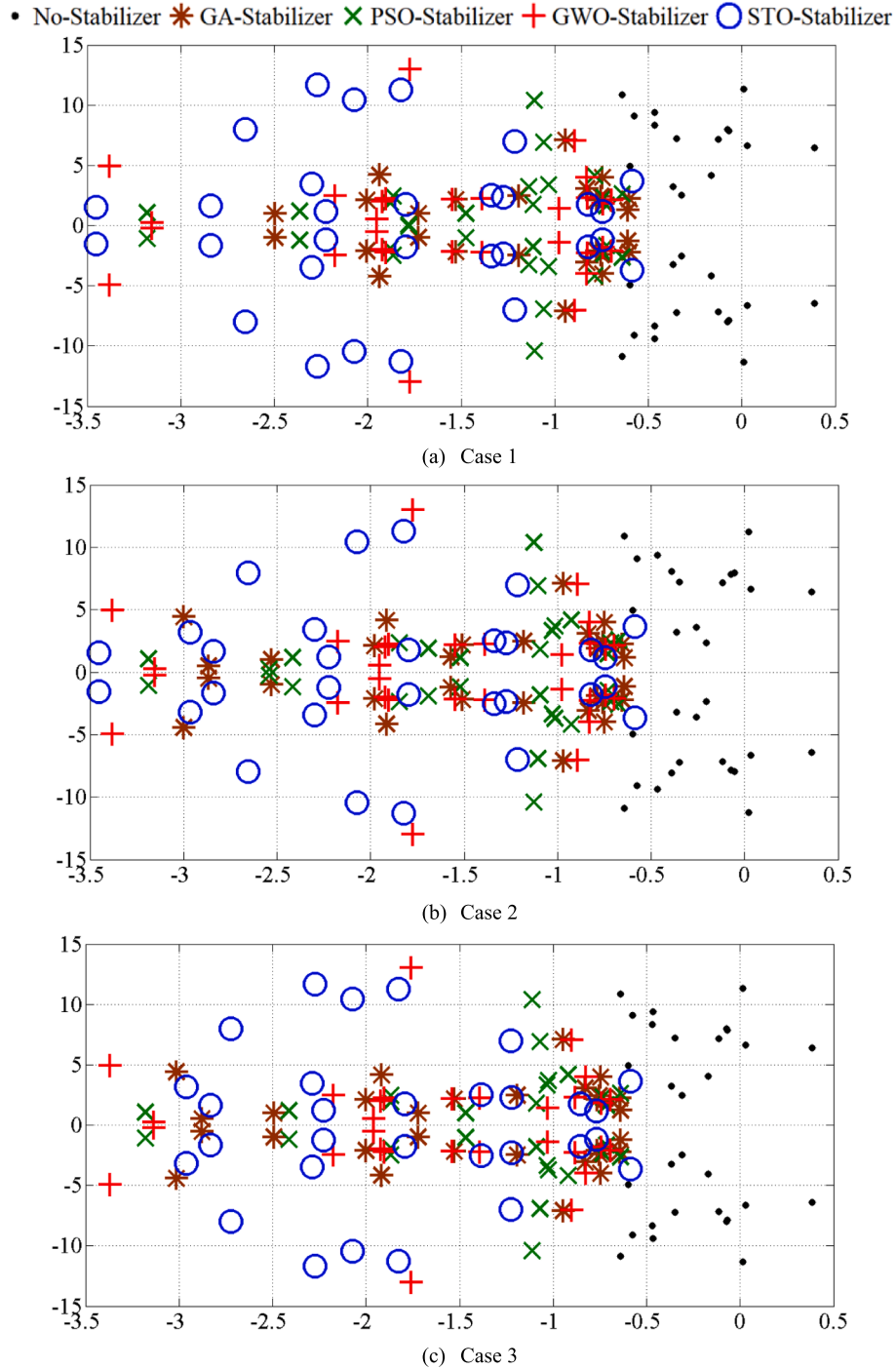


Fig. 5. Eigenvalue Map analysis with No-PSS and Designed PSS for six operating cases of NEEPG System.

of WSCC system and NEEPG system with No-PSS and GA-stabilizer, PSO-stabilizer, GWO-stabilizer and STO-stabilizer are depicted in Figs. 4 and 5 for selected operating cases respectively.

It is clear from Tables 9 and 10, Figs. 4 and 5 that eigenvalues of the designed GWO-stabilizer and STO-stabilizer are not only repositioned from the unstable and/or lightly damped oscillations zone to significantly far away from a selected D-shape stable zone in the s -plane but also shift other oscillation modes to the left-half of s -plane as compared to same obtained by GA-stabilizer and PSO-stabilizer for selected operating cases of WSCC and NEEPG systems respectively. From the outcomes, it is clear that the damping performance of the stabilizer planned

using the STO-stabilizer is better than the stabilizers planned using GA, PSO, and GWO techniques.

4.5. Simulation results

To analyse the performance of the planned STO-stabilizer described in section 4.4 for WSCC and NEEPG systems, decisive perturbations are selected, and their performance is matched with the performance of GA-stabilizer, PSO-stabilizer, and GWO-stabilizer. The results are shown in Table 11.

The responses of the generator speed deviations Δw_{12} , Δw_{23} , and

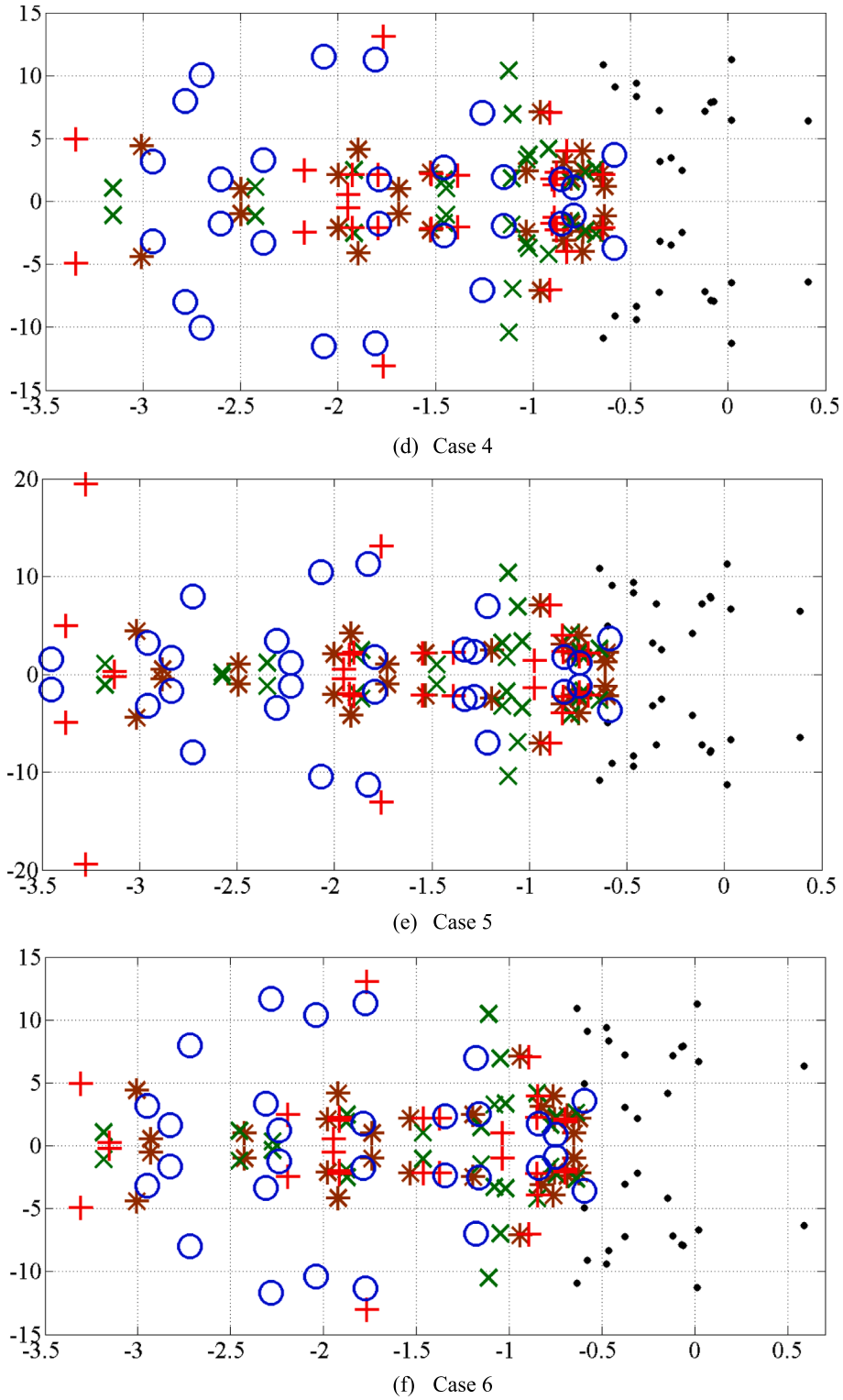


Fig. 5. (continued).

Table 11
Critical Perturbation for Testing the Performance of Planned PSS.

Strategies	Most Critical Disturbances
Strategy-1	A 6-cycle, 3-phase short circuit fault occur at $t = 1$ sec on bus 7 by tripping the lines 5–7 of the WSCC system
Strategy-2	A 6-cycle, 3-phase short circuit fault occur at $t = 1$ sec on bus 21 without tripping the lines 21–22 of the NEEPG system

Δw_{31} without employing PSS for Strategy-1 of heavy loading case of WSCC system and all sixteen generator speed deviations for Strategy-2 of critical operating Case-6 of NEEPG system are illustrated in Figs. 6 (a) and 7 (a) respectively whereas for the same strategies with planned GA-stabilizer, PSO-stabilizer, GWO-stabilizer and STO-stabilizer, generator speed deviations Δw_{12} , Δw_{23} and Δw_{31} of WSCC system and critical generator speed deviations Δw_5 , Δw_6 and Δw_9 of NEEPG system are illustrated in Figs. 6 (b)–(d) and 7 (b)–(d) respectively.

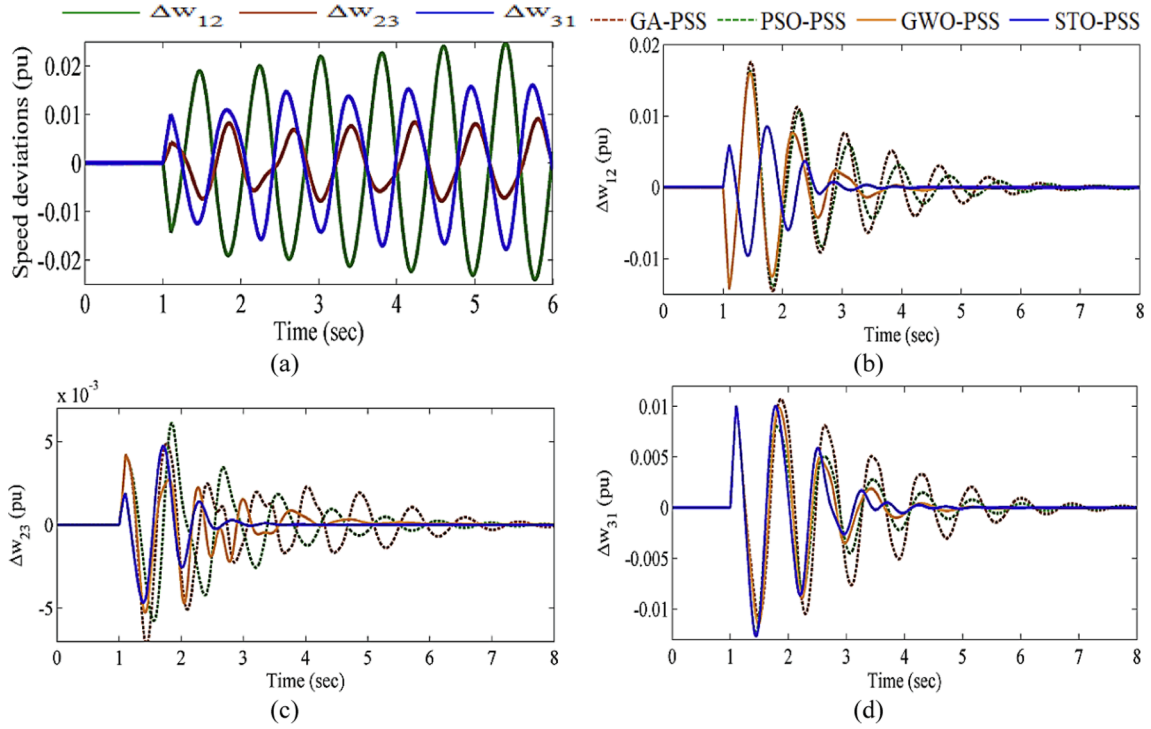


Fig. 6. Generator speed deviations (a) without-PSS and (b) Δw_{12} (c) Δw_{23} (d) Δw_{31} with GA-stabilizer, PSO-stabilizer, GWO-stabilizer, and STO-stabilizer for Strategy-1 of heavy loading case for WSCC system.

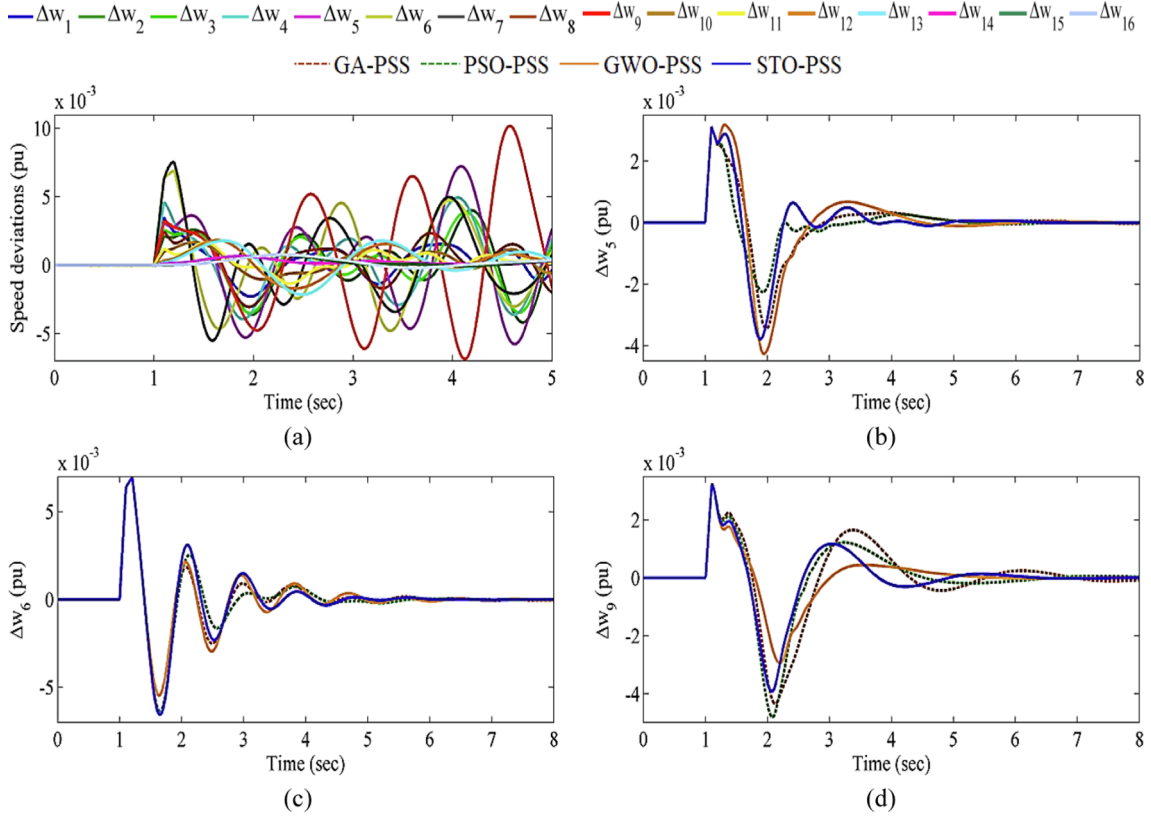


Fig. 7. Generator speed deviations (a) without PSS and (b) Δw_5 (c) Δw_6 , (d) Δw_9 with GA-stabilizer, PSO-stabilizer, GWO-stabilizer, and STO-stabilizer for Strategy-2 of operating Case-6 of NEEPG system.

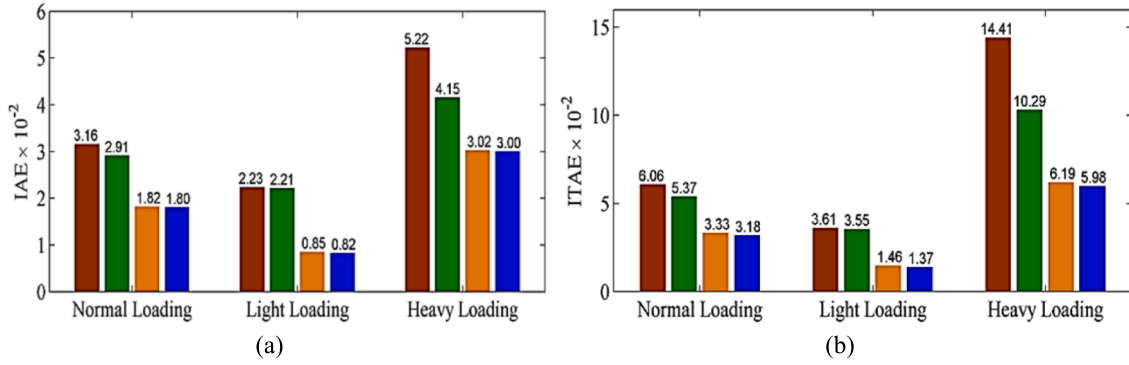


Fig. 8. Comparison of performance indices (a) *IAE* (b) *ITAE* for three loading cases of WSCC system with Designed GA-stabilizer, PSO-stabilizer, GWO-stabilizer, and STO-stabilizer.

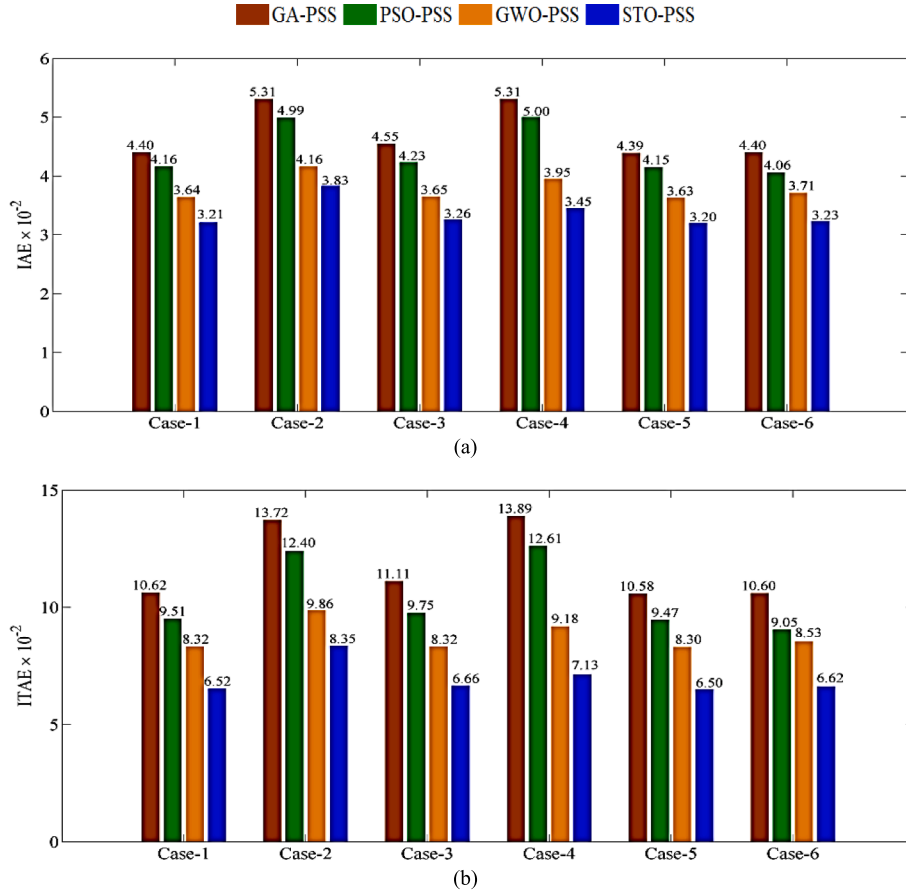


Fig. 9. Comparison of performance indices (a) *IAE* (b) *ITAE* for six operating cases of NEEPG system with Designed GA-stabilizer, PSO-stabilizer, GWO-stabilizer, STO-stabilizer.

On comparison of Figs. 6 (a) and 7 (a), it is clear that with the increment of load, the size and duration of oscillations of all three generators increase in the same direction and are oscillatory in nature, and finally all generators lose synchronism. Furthermore, it is noticed from Figs. 6 (b)-(d) and 7 (b)-(d) that speed deviations for all generators with planned GWO-stabilizer and STO-stabilizer show fast decaying of oscillations, settle fast and improve the relative stability as compared to other techniques. Furthermore, the performance of the planned STO-stabilizer is comparable with GWO-stabilizer and superior to GA-stabilizer and PSO-stabilizer.

A comparison of performance indices *IAE* and *ITAE* as bar-charts with designed GA-stabilizer, PSO-stabilizer, GWO-stabilizer, and STO-

stabilizer for Strategy-1 of WSCC system and Strategy-2 of NEEPG system are depicted in Figs. 8 (a)-(b) and 9 (a)-(b) respectively.

These bar-charts indicate that the performance of the STO-stabilizer is better than the other three stabilizers for the selected decisive perturbation for both strategies. The performance of the GWO-stabilizer and STO-stabilizer is almost similar for time domain specifications. Furthermore, it may be concluded that local-area and inter-area modes have been well stabilized with less overshoot, peak values, and settling time using all planned PSS under selected decisive perturbations [47].

Table 12
Three Hidden Operating Conditions of WSCC Power System [47].

Operating Cases		Generator			Load		
		G_1	G_2	G_3	A	B	C
Hidden Case-I	P	0.33	2.00	1.50	1.50	1.20	1.00
	Q	1.12	0.57	0.38	0.90	0.80	0.50
Hidden Case-II	P	1.09	2.45	1.27	1.90	1.30	1.50
	Q	0.79	0.57	0.21	0.75	0.45	0.50
Hidden Case-III	P	1.41	2.60	1.20	2.00	1.50	1.60
	Q	0.59	0.38	0.02	0.60	0.30	0.20

Table 13
Three Hidden Operating Conditions of the NEEPG System.

Cases	Operating Conditions
Hidden Case-1	Total real and reactive power enhanced by 25 %
Hidden Case-2	Total real and reactive power reduced by 15 %
Hidden Case-3	Transmission lines 1–31, 10–11, 30–32, and 33–34 are out of service

5. Robustness performance analysis

In sub-section 4.5, it is depicted that the planned GWO-stabilizer and STO-stabilizer are more effective than the PSS design using GA and PSO techniques. Therefore, to examine the impact of robustness performance of GA-stabilizer, PSO-stabilizer, GWO-stabilizer, and STO-stabilizer on WSCC and NEEPG systems; three hidden cases of WSCC [51] and NEEPG systems are selected, and the operating conditions chosen are illustrated in Tables 12 and 13 respectively.

In this section comparison of planned GWO-stabilizer, STO-stabilizer with GA-stabilizer, and PSO-stabilizer is done based on eigenvalue analysis, performance indices, and nonlinear simulation results. The eigenvalue analysis detail data without PSS for unstable and/or

marginally stable mechanical modes of WSCC [51] and NEEPG systems are illustrated in Tables 14 and 15 respectively. Eigenvalue map analysis of WSCC system and NEEPG system with No-PSS and GA-stabilizer, PSO-stabilizer, GWO-stabilizer, and STO-stabilizer are depicted in Figs. 10 (a)–(c) and 11 (a)–(c) for selected hidden operating cases respectively.

From Table 14, it is seen that one-pair of eigenvalues without-PSS fall in the unstable sector of the s -plane and have a negative damping ratio for all chosen hidden operating cases of the WSCC system. Moreover, the hidden operating Case-3 is extremely unstable due to a high negative percentage damping ratio compared to other hidden cases as well as the previous three operating cases for which the PSS are planned. From Table 15, it is seen that the NEEPG system is unstable with two, two, and five pairs of eigenvalues without-PSS for hidden operating cases 1, 2, and 3 respectively and they lie in the unstable zone of the s -plane with negative percentage damping ratio. The hidden operating Case-3 is highly unstable due to a larger negative percentage damping ratio as compared to other hidden operating cases as well as for six-operating cases studied earlier.

Eigenvalues and percentage damping ratio with earlier planned PSS using GA, PSO, GWO, and STO techniques for three hidden operating cases of WSCC and NEEPG systems are evaluated using PSAT [45] and are listed in Tables 16 and 17 respectively.

On analysing Tables 16 and 17, Figs. 10 and 11, it is revealed that with planned GWO-stabilizer and STO-stabilizer, the eigenvalues are relocated far away from the selected D-shape stable sector in the s -plane with superior damping performance as compared to PSS planned using GA and PSO techniques and ensure dynamic stability for all selected hidden operating cases also.

To illustrate the impact of the robustness performance of STO-stabilizer for selected hidden operating cases for WSCC and NEEPG systems, decisive perturbations listed in Table 11 are selected for testing their simulation performance and compared with without stabilizer, GA-stabilizer, PSO-stabilizer, and GWO-stabilizer. Fig. 12 (a) illustrates the responses of generator speed deviations Δw_{12} , Δw_{23} and Δw_{31} with No-PSS for Strategy-1 of decisive hidden operating Case-3 of WSCC and Fig. 13 (a) shows all generator speed deviations with No-PSS for Strategy-2 of decisive hidden operating Case-3 of NEEPG system

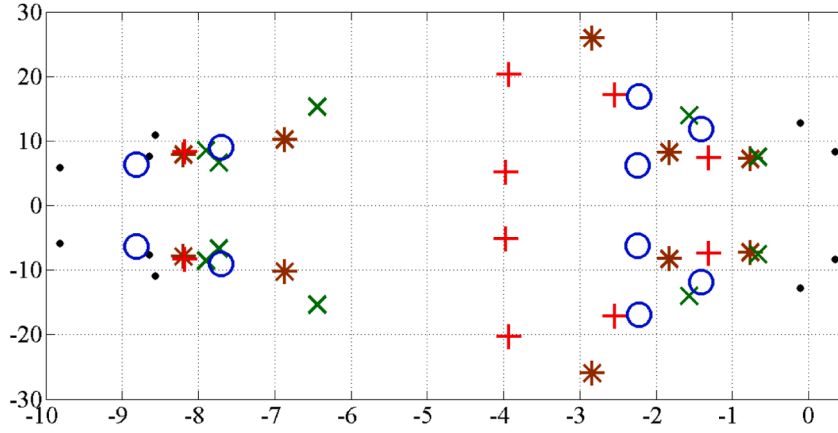
Table 14
Eigenvalues Analysis without PSS for Three Hidden Operating Cases of WSCC System.

	Eigenvalues	Damping Ratio (%)	Frequency (p. u.)	Participation Factor	Participation Modes
Hidden Case-1	$0.341 \pm j 8.339$	– 4.00	1.327	0.269	w_2, δ_2
	$-0.109 \pm j 12.803$	0.85	2.037	0.363	w_3, δ_3
Hidden Case-2	$0.465 \pm j 8.357$	– 5.50	1.330	0.272	w_2, δ_2
	$-0.250 \pm j 12.931$	1.90	2.058	0.382	w_3, δ_3
Hidden Case-3	$0.604 \pm j 8.375$	– 7.20	1.333	0.270	w_2, δ_2
	$-0.233 \pm j 12.981$	8.00	2.065	0.383	w_3, δ_3

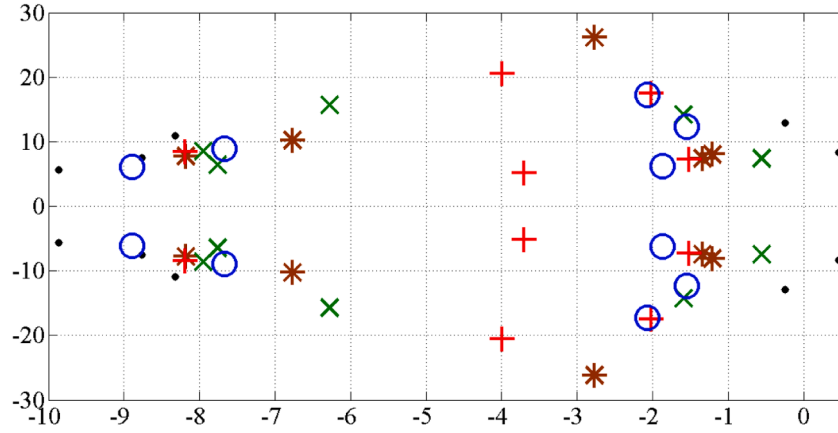
Table 15
Eigenvalues Analysis without PSS for Three Hidden Operating Cases of NEEPG System.

	Eigenvalues	Damping Ratio (%)	Frequency (p.u.)	Participation Factor	Participation Modes
Hidden Case-1	$0.310 \pm j 6.418$	– 4.83	1.021	0.345	w_9, δ_9
	$0.0005 \pm j 6.628$	– 0.008	1.055	0.185	w_2, δ_2
Hidden Case-2	$0.406 \pm j 6.425$	– 6.31	1.022	0.347	w_9, δ_9
	$0.035 \pm j 6.610$	– 0.54	1.052	0.188	w_2, δ_2
Hidden Case-3	$0.386 \pm j 6.420$	– 5.99	1.021	0.352	w_9, δ_9
	$0.329 \pm j 5.485$	– 5.99	0.873	0.350	w_{11}, δ_{11}
	$0.038 \pm j 6.661$	– 0.57	1.060	0.235	w_2, δ_2
	$0.013 \pm j 7.368$	– 0.18	1.172	0.165	w_2, δ_2
	$0.003 \pm j 8.090$	– 0.03	1.287	0.374	w_{10}, δ_{10}

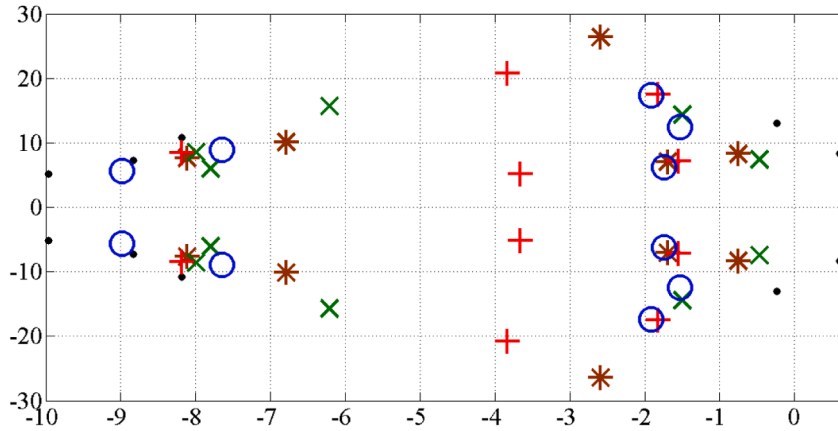
- No-Stabilizer * GA-Stabilizer x PSO-Stabilizer + GWO-Stabilizer o STO-Stabilizer



(a) Hidden Case-1 of WSCC System



(b) Hidden Case-2 of WSCC System



(c) Hidden Case-3 of WSCC System

Fig. 10. Eigenvalue Map analysis with No-PSS and Designed PSS for hidden operating cases of (a)-(c) WSCC system.

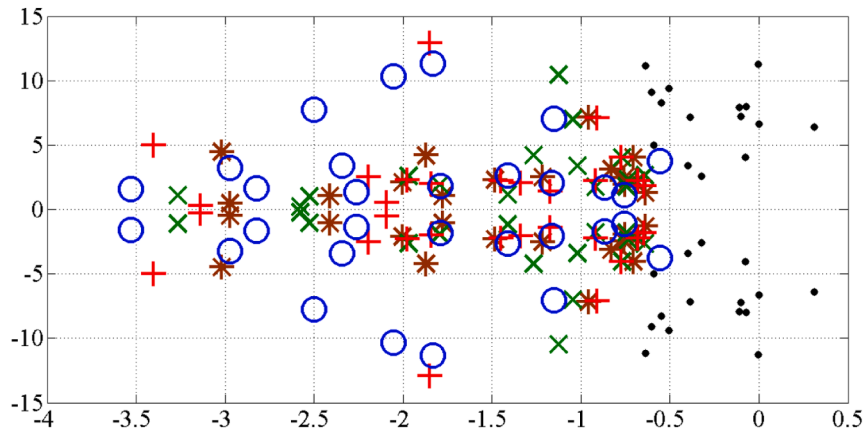
whereas, for the same hidden operating cases, speed deviations Δw_{12} , Δw_{23} , and Δw_{31} with planned GA-stabilizer, PSO-stabilizer, GWO-stabilizer, and STO-stabilizer provided with WSCC system are illustrated in Fig. 12 (b)-(d) and critical generator speed deviations Δw_5 , Δw_6 and Δw_9 of NEEPG system are depicted in Fig. 13 (b)-(d) respectively.

From Figs. 12 (a) and 13 (a), it is clear that with a decisive line outage, the amplitude and duration of oscillations for all three generators increase indefinitely and finally lose synchronism. Fig. 12 (b)-(d)

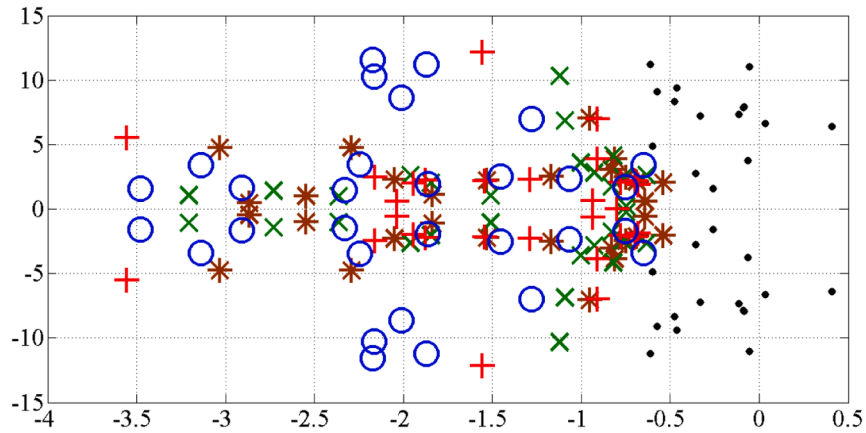
and 13 (b)-(d), it is noticed that system provided with planned GWO-stabilizer and STO-stabilizer, oscillations die down quickly thus improving the relative stability as compared to GA-stabilizer and PSO-stabilizer.

To test the robust performance of the planned STO-stabilizer, a comparison of performance indices: IAE and $ITAE$ are evaluated and plotted as bar-charts for Strategy-1 of the WSCC system and Strategy-2 of NEEPG system in Figs. 14 (a)-(b) and 15 (a)-(b) respectively. It is

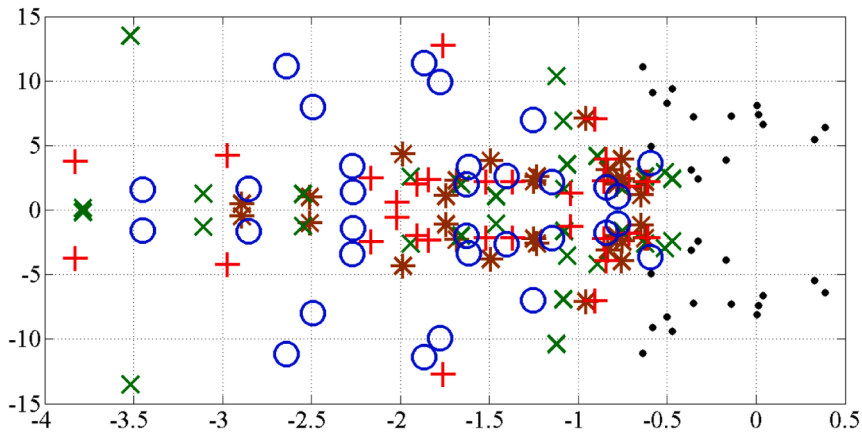
- No-Stabilizer * GA-Stabilizer x PSO-Stabilizer + GWO-Stabilizer o STO-Stabilizer



(a) Hidden Case-1 of NEEPG System



(b) Hidden Case-2 of NEEPG System



(c) Hidden Case-3 of NEEPG System

Fig. 11. Eigenvalue Map analysis with No-PSS and Designed PSS for hidden operating cases of (a)-(c) NEEPG system.

Table 16

Eigenvalues Analysis with Planned PSS for Three Hidden Operating Cases of WSCC System.

	Hidden Case-1	Hidden Case-2	Hidden Case-3
With GA-stabilizer [47]	$-0.766 \pm j 7.225$, 10.5 % $-1.829 \pm j 8.273$, 21.5 %	$-1.228 \pm j 8.052$, 15.0 % $-1.327 \pm j 7.440$, 17.5 %	$-0.746 \pm j 8.283$, 8.9 % $-2.587 \pm j 26.412$, 9.7 %
With PSO-stabilizer [47]	$-0.664 \pm j 7.530$, 8.7 % $-1.565 \pm j 13.977$, 11.1 %	$-0.557 \pm j 7.442$, 7.4 % $-1.587 \pm j 14.234$, 11.0 %	$-0.465 \pm j 7.442$, 6.2 % $-1.495 \pm j 14.387$, 10.3 %
With GWO-stabilizer [47]	$-1.311 \pm j 7.403$, 17.4 % $-2.538 \pm j 17.182$, 14.6 %	$-1.516 \pm j 7.229$, 20.5 % $-2.017 \pm j 17.487$, 11.4 %	$-1.547 \pm j 7.106$, 21.2 % $-1.825 \pm j 17.495$, 10.3 %
With STO-stabilizer	$-1.413 \pm j 11.853$, 11.8 % $-2.220 \pm j 16.966$, 12.9 %	$-1.553 \pm j 12.297$, 12.5 % $-2.065 \pm j 17.316$, 11.8 %	$-1.527 \pm j 12.467$, 12.1 % $-1.913 \pm j 17.369$, 10.9 %

Table 17

Eigenvalues Analysis with Planned PSS for Three Hidden Operating Cases of NEEPG System.

Cases	With GA-stabilizer	With PSO-stabilizer	With GWO-stabilizer	With STO-stabilizer
Hidden Case-1	$-0.688 \pm j 2.229$, 29.5 % $-0.706 \pm j 4.035$, 17.2 %	$-0.640 \pm j 2.649$, 23.5 % $-0.768 \pm j 4.029$, 18.7 %	$-0.681 \pm j 2.208$, 29.5 % $-0.773 \pm j 4.028$, 18.8 %	$-0.557 \pm j 3.771$, 29.5 % $-1.153 \pm j 7.027$, 16.1 %
Hidden Case-2	$-0.953 \pm j 7.048$, 13.4 % $-0.810 \pm j 3.862$, 20.5 % $-0.539 \pm j 2.032$, 25.6 %	$-1.121 \pm j 10.319$, 10.8 % $-0.818 \pm j 4.148$, 19.3 % $-0.633 \pm j 2.642$, 23.3 %	$-1.556 \pm j 12.160$, 12.6 % $-0.910 \pm j 7.001$, 12.8 % $-0.696 \pm j 2.174$, 30.4 %	$-1.280 \pm j 6.965$, 18.0 % $-0.651 \pm j 3.415$, 18.7 % $-0.754 \pm j 1.702$, 40.5 %
Hidden Case-3	$-0.956 \pm j 7.077$, 13.3 % $-0.754 \pm j 7.084$, 18.6 % $-0.831 \pm j 3.084$, 26.0 % $-0.750 \pm j 2.434$, 29.4 % $-0.624 \pm j 2.188$, 27.4 %	$-1.123 \pm j 10.385$, 10.7 % $-1.085 \pm j 6.919$, 15.5 % $-0.891 \pm j 4.181$, 20.8 % $-0.512 \pm j 2.937$, 17.1 % $-0.472 \pm j 2.416$, 19.1 %	$-1.761 \pm j 12.765$, 13.6 % $-0.905 \pm j 7.035$, 12.7 % $-0.842 \pm j 3.995$, 20.8 % $-0.855 \pm j 2.226$, 35.8 % $-0.606 \pm j 2.177$, 26.8 %	$-1.868 \pm j 11.366$, 16.2 % $-1.256 \pm j 6.988$, 17.6 % $-1.777 \pm j 9.915$, 17.6 % $-0.842 \pm j 1.753$, 43.2 % $-0.593 \pm j 3.623$, 16.1 %

clear from Figs. 14 and 15, that the numerical values of both indices for systems provided with planned STO-stabilizer are lowest as compared to GA-stabilizer, PSO-stabilizer, and GWO-stabilizer for decisive perturbations of three hidden operating cases.

It can also be concluded that local-area and inter-area modes have been well stabilized with less overshoot, peak values, and settling time using all planned PSSs for both chosen loading cases as well as hidden operating cases of WSCC and NEEPG systems.

6. Conclusion and future scope

This paper offering a comparative analysis of bio-inspired meta-heuristic optimization techniques: STO, GWO, PSO, and GA for designing robust PSS for the MMPS. The tuning method is considered a multi-objective optimization problem for relocating unstable right-half of s -plane eigenvalues to a definite stable D-shape sector in the left-half of the s -plane. To check the performance of the designed PSS, these techniques are effectively tested on two benchmark test systems: sixteen-machine, sixty-eight-bus New England Extended Power Grid (NEEPG) and three-machine, nine-bus Western System Coordinating Council (WSCC) for an extensive variety of operating conditions under critical perturbations. The superiority of the STO-stabilizer is revealed by analyzing its performance using non-linear simulations, performance indices, and eigenvalue analysis and by comparing it with GA-stabilizer, PSO-stabilizer, and GWO-stabilizer. The results prove that the designed STO-stabilizer produces better damping performance for a wide range of operating conditions as well as for hidden operating cases under critical disturbance as compared to others. This research work can also be extended to advance coordinated tuning of PSS parameters with

different shunt and series FACTS damping controllers for improving the small-signal stability of power systems.

CRediT authorship contribution statement

Dhanraj Chitara: Conceptualization, Formal analysis, Investigation, Visualization, Writing – original draft, Writing – review & editing. **P.K. Singhal:** Investigation, Visualization, Writing – original draft, Writing – review & editing. **S.L. Surana:** Investigation, Visualization, Writing – original draft, Writing – review & editing. **Gulshan Sharma:** Data curation, Methodology, Supervision, Writing – review & editing. **R.C. Bansal:** Conceptualization, Data curation, Methodology, Project administration, Supervision, Validation.

Declaration of Competing Interest

The authors declare that they have no known competing financial interests or personal relationships that could have appeared to influence the work reported in this paper.

Data availability

Data will be made available on request.

Appendix

Static exciter for WSCC system: $K_a = 100$, $T_a = 0.05$ sec, for NEEPG system: $K_a = 50$, $T_a = 0.001$ sec

The control parameters of GA, PSO, GWO and STO algorithm are

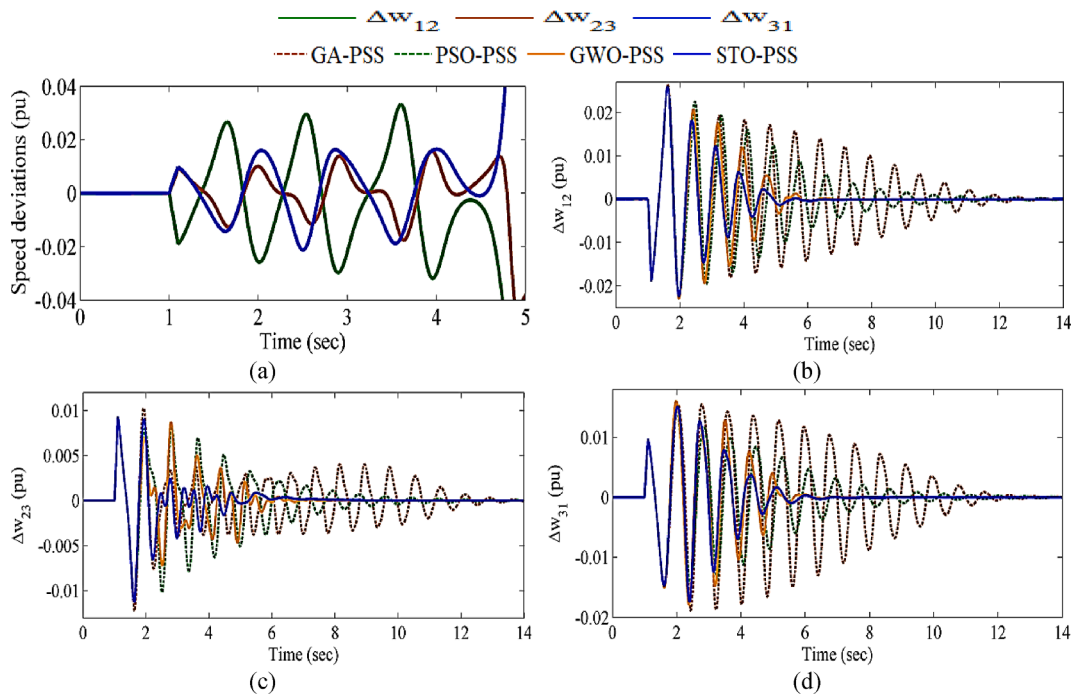


Fig. 12. Generator speed deviations (a) without-PSS and (b) Δw_{12} (c) Δw_{23} (d) Δw_{31} with GA-stabilizer, PSO-stabilizer, GWO-stabilizer, and STO-stabilizer for Strategy-1 of hidden operating Case-3 of WSCC system.

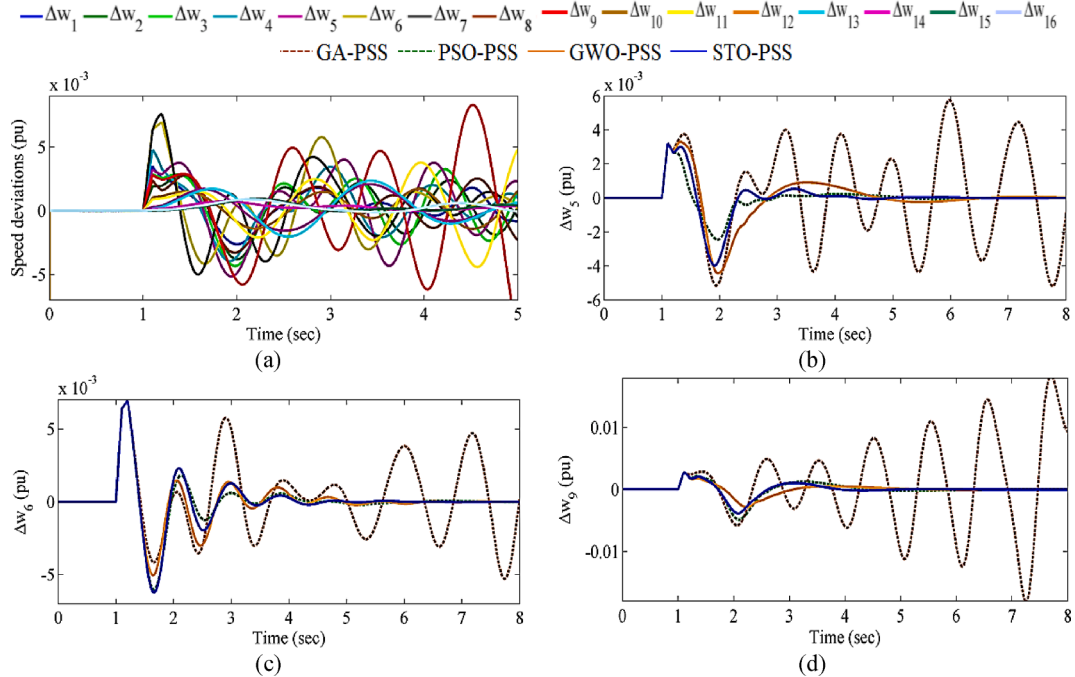


Fig. 13. Generator speed deviations (a) without-PSS and (b) Δw_5 (c) Δw_6 (d) Δw_9 with GA-stabilizer, PSO-stabilizer, GWO-stabilizer and STO-stabilizer for Strategie-2 of hidden operating Case-3 of NEEPG system.

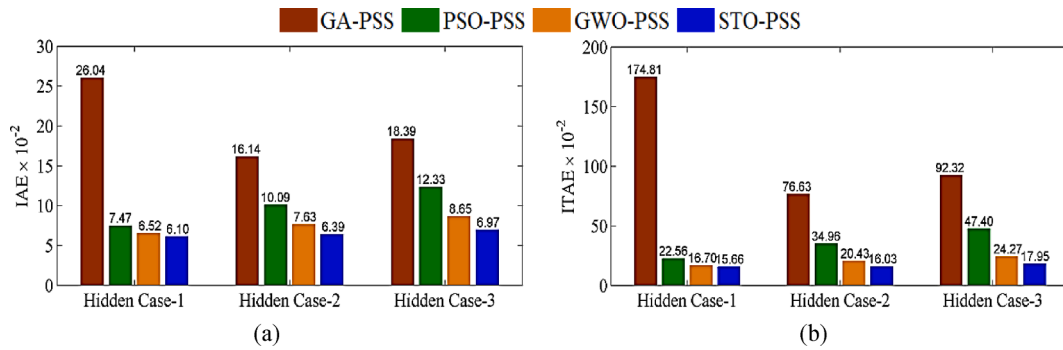


Fig. 14. Comparison of performance indices (a) IAE and (b) ITAE for Strategy-1 with GA-stabilizer, PSO-stabilizer, GWO-stabilizer, and STO-stabilizer for hidden operating cases 1–3 of WSCC system.

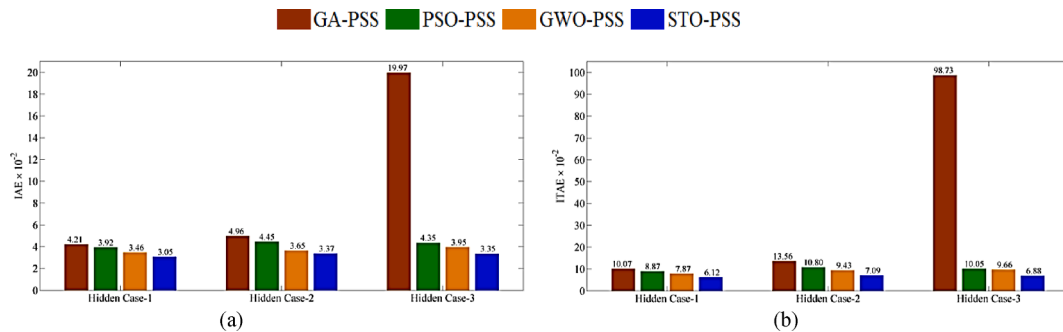


Fig. 15. Comparison of performance indices (a) IAE and (b) ITAE for Strategy-2 with GA-stabilizer, PSO-stabilizer, GWO-stabilizer, and STO-stabilizer for hidden operating cases 1–3 of NEEPG system.

given by:

Population = 70, Number of iteration = 70, Number of individuals = 06 (WSCC System)

Population = 100, Number of iteration = 100, Number of individuals = 42 (NEEPG System).

GA: Crossover rate = 0.75 (WSCC System), 0.80 (NEEPG System), Mutation rate = 0.01

PSO: c_1 , $c_2 = 2$, $w_{min} = 0.4$, $w_{max} = 0.9$

GWO: $a = [2, 0]$, $A = [-2a, 2a]$, $C = [0, 2]$

STO: $S_a = [2, 0]$, $C_B = 0.5R$, where $R = [0, 1]$

References

- [1] Kundur P. Power System Stability and Control. Edited by Neal J. Balu, and Mark G. Lauby 4.2 1994.
- [2] Kundur P, et al. Definition and Classification of Power System Stability IEEE/CIGRE Joint Task Force on Stability Terms and Definitions. IEEE Trans Power Syst 2004;19(3):1387–401.
- [3] Demello FP, Concordia C. Concepts of Synchronous Machine Stability as Affected By Excitation Control. IEEE Trans Power Syst 1969;88(4):316–29.
- [4] Bollinger K, et al. Power Stabilizer Design Using Root Locus Methods. IEEE Trans Power Syst 1975;94(5):1484–8.
- [5] Bollinger KE, Winsor R, Campbell A. Frequency Response Methods for Tuning Stabilizers to Damp Out Tie-Line Power Oscillations: Theory and Field-Test Results. IEEE Trans Power Syst 1979;PAS-98(5):1509–15.
- [6] DeMello FP, et al. A Power System Stabilizer Design Using Digital Control. IEEE Trans Power Syst 1982;8:2860–8.
- [7] Shrikant Rao P, Sen I. Robust Pole Placement Stabilizer Design Using Linear Matrix Inequalities. IEEE Trans Power Syst 2000;15(1):313–9.
- [8] Chen S, Malik OP. H_∞ Based Power System Stabilizer Design. IEE Proc Gener Transm Distr March 1995;142(2):179–84.
- [9] Shah R, Mithulananthan N, Lee KY, Bansal RC. Wide-Area Measurement Signal-Based Stabilizer For Large-Scale Photovoltaic Plants With High Variability And Uncertainty. IET-Renew Power Gener 2013;7(6):614–22.
- [10] Kamalasadan S, Swann GD, Yousefian R. A Novel System-Centric Intelligent Adaptive Control Architecture for Power System Stabilizer Based On Adaptive Neural Networks. IEEE Syst J Dec. 2014;8(4):1074–85.
- [11] Chopra R, Joshi D, Bansal RC. Analysis Delta-Omega and Fuzzy Logic Power System Stabilizer Performances under Several Operating Conditions. J Renew Sustain Energy 2009;1(3):1–11.
- [12] Radaideh SM, Nejdawi IM, Mushtaha MH. Design Of Power System Stabilizers Using Two-Level Fuzzy And Adaptive Neuro-Fuzzy Inference Systems. Int J Electr Power Energy Syst 2012;35(1):47–56.
- [13] Abdel-Magid YL, Dawoud MM. Tuning of power system stabilizers using genetic algorithms. Electr Pow Syst Res 1996;39(2):137–43.
- [14] Abido MA. A Novel Approach to Conventional Power System Stabilizer Design Using Tabu Search. Int J Electr Power Energy Syst 1999;21(6):443–54.
- [15] Abido MA. Robust Design Of Multi-Machine Power System Stabilizers Using Simulated Annealing. IEEE Trans Energy Convers 2000;15(3):297–304.
- [16] Abido MA. Optimal Design of Power-System Stabilizers Using Particle Swarm Optimization. IEEE Trans Energy Convers 2002;17(3):406–13.
- [17] Abido MA, Abdel-Magid YL. Optimal Design of Power System Stabilizer Using Evolutionary Programming. IEEE Transactions Energy Conversions Sep. 2002;17(4):429–36.
- [18] Mishra S, Tripathy M, Nanda J. Multi-Machine Power System Stabilizer Design By Rule-Based Bacteria Foraging. Electr Pow Syst Res 2007;77(12):1595–607.
- [19] Shayeghi H, Shayanfar HA, Jalilzadeh S, Safari A. Multi-Machine Power System Stabilizers Design Using Chaotic Optimization Algorithm. Energy Convers Manage March 2010;51:1572–80.
- [20] Linda MM, Nair NK. Optimal Design of Multi-Machine Power System Stabilizer Using Robust Ant Colony Optimization Technique. Trans Inst Meas Control 2012;34(7):829–40.
- [21] Khodabakhshian A, Hemmati R. Multi-Machine Power System Stabilizers Design By Using Cultural Algorithms. Int J Electr Power Energy Syst Sep. 2013;44:571–80.
- [22] Ali ES. Optimization of Power System Stabilizers Using BAT Search Algorithm. Int J Electr Power Energy Syst 2014;61:683–90.
- [23] Eke İ, Taplamacıoğlu MC, Lee KY. Robust Tuning Of Power System Stabilizer by Using Orthogonal Learning Artificial Bee Colony. IFAC-Papers online 2015;48(30):149–54.
- [24] Farah A, Guesmi T, Abdallah HH, Ouali A. A Novel Chaotic Teaching–Learning–Based Optimization Algorithm for Multi-Machine Power System Stabilizers Design Problem. Int J Electr Power Energy Syst 2016;75:197–209.
- [25] Abd Elazim SM, Ali ES. Optimal Power System Stabilizers Design Via Cuckoo Search Algorithm. Int J Electr Power Energy Syst 2016;75:99–107.
- [26] Islam NN, Hannan MA, Shareef H, Mohamed A, Azah Mohamed. “An Application of Backtracking Search Algorithm in Designing Power System Stabilizers for Large Multi-Machine System. Neurocomputing 2017;237:175–84.
- [27] Serdar E, Hekimoglu B. Parameter Optimization of Power System Stabilizer via Salp Swarm Algorithm. 5th IEEE International Conference on Electrical and Electronic Engineering (ICEEE). 2018.
- [28] Spoljarić T, Pavić I. Performance analysis of an ant lion optimizer in tuning generators' excitation controls in multi machine power system. 41st IEEE International Convention on Information and Communication Technology, Electronics and Microelectronics (MIPRO). 2018.

- [29] Meysam R, Seyedtabaai S. Multi-machine optimal power system stabilizers design based on system stability and nonlinearity indices using Hyper-Spherical Search method. *Int J Electr Power Energy Syst* 2019;105:729–40.
- [30] Serdar E, et al. An Application of Slime Mould Algorithm for Optimizing Parameters of Power System Stabilizer. 4th IEEE International Symposium on Multidisciplinary Studies and Innovative Technologies (ISMSIT). 2020.
- [31] Ekinci S, Izci D, Hekimoglu B. Implementing the Henry Gas Solubility Optimization Algorithm for Optimal Power System Stabilizer Design. *Electrica* 2021;21(2): 250–8.
- [32] Chaib L, Choucha A, Arif S, Zaini HG, El-Fergany A, Ghoneim SSM. Robust Design Of Power System Stabilizers Using Improved Harris Hawk Optimizer For Interconnected Power System. *Sustainability* Oct. 2021;13(21):11776.
- [33] Serdar E, et al. Development of Lévy Flight-Based Reptile Search Algorithm with Local Search Ability for Power Systems Engineering Design Problems. *Neural Comput & Applic* 2022;34(22):20263–83.
- [34] Davut I. A novel improved atom search optimization algorithm for designing power system stabilizer. *Evol Intel* 2022;15(3):2089–103.
- [35] Boucetta I, Naimi D, Salhi A, Abujarad S, Zellouma L. Power System Stability Enhancement Using A Novel Hybrid Algorithm Based On The Water Cycle Moth-Flame Optimization. *Energies* 2022;15(14):1–17.
- [36] Moghadam AT, Aghahadi M, Eslami M, Rashidi S, Arandian B, Nikolovski S. Adaptive Rat Swarm Optimization For Optimum Tuning Of SVC And PSS In A Power System. *Int Trans Electr Energy Syst* Jan. 2022;2022:1–13.
- [37] Grace SS, Kumaravel S, Ashok S. Revamped Sine Cosine Algorithm Centered Optimization of System Stabilizers and Oscillation Dampers for Wind Penetrated Power System. *IEEE Access* 2022;11:1890–905.
- [38] Snásel V, et al. Weighted Mean of Vectors Optimization Algorithm and its Application in Designing the Power System Stabilizer. *Appl Soft Comput* 2023;136 (110085):pp.
- [39] Ruswandi DM, Robandi I, Prakasa MA. Stability Enhancement of Sulselrabar Electricity System Using Mayfly Algorithm Based on Static Var Compensator and Multi-Band Power System Stabilizer PSS2B. *IEEE Access* 2023;11:57319–40.
- [40] El-Dabah MA, Hassan MH, Kamel S, Zawbaa HM. Robust Parameters Tuning Of Different Power System Stabilizers Using A Quantum Artificial Gorilla Troops Optimizer. *IEEE Access* 2022;10:82560–79.
- [41] Dhiman G, Kaur A. STOA: A Bio-Inspired Based Optimization Algorithm for Industrial Engineering Problems. *Eng Appl Artif Intel* Jun 2019;82:148–74.
- [42] Mirjalili S, Mirjalili SM, Lewis A. Grey Wolf Optimizer. *Adv Eng Softw* March 2014; 69:46–61.
- [43] Goldberg DE. Genetic algorithms in search, optimization and machine learning. Addison-Wesley; 1989.
- [44] Kennedy J, Eberhart RC. Particle Swarm Optimization. In: *Proc. IEEE International Conference on Neural Networks*, Piscataway, NJ, vol. IV, pp. 1942–1948, 1995.
- [45] Milano F. *Power System Analysis Toolbox Manual-Documentation for PSAT* Version 2.1. 6. Univ Coll Dublin, Dublin Irel Tech Rep 2010.
- [46] Anderson PM, Fouad AA. *Power System Control and Stability*, ISBN-9780470545577, Piscataway, NJ: IEEE Press, 2nd Edition, 2003.
- [47] Sharma RK, Chitara D, Raj S, Niazi KR, Swarnkar A. Multi-machine Power System Stabilizer Design Using Grey Wolf Optimization. In: *Proceedings of International Conference on Computational Intelligence and Emerging Power System*, pp. 331–343, Springer, Singapore, 2022.
- [48] Rogers G. *Power system oscillations*. Springer; 1999.
- [49] Shayeghi H, Ghasemi A. A multi objective vector evaluated improved honey bee mating optimization for optimal and robust design of power system stabilizers. *International Journal of Electrical Power & Energy Systems* May 2014;62:630–45.
- [50] Hsu YY, Chen CL. Identification of optimum location for stabilizer applications using participation factors. *IEE Proc C Gener Transm and Distr* May 1987;134(3): 238–44.
- [51] Chitara D, Meena NK, Yang J, Niazi KR, Swarnkar A, Gupta N, Vega-Fuentes E. Small-Signal Stability Enhancement of Multi-Machine Power System Using Cuckoo and Harmony Search Optimization Techniques, In: *Vol. 05: Proceedings of 11th International Conference on Applied Energy, Part 4*, Sweden, pp. 1–6, Aug. 2019.